1963

Excitation temperatures of arc discharges in inert gas atmosopheres

James Olaf Tveekrem
Iowa State University

EXCITATION TEMPERATURES OF ARC DISCHARGES IN INERT GAS ATMOSPHERES

by

James Olaf Tveekrem

A Dissertation Submitted to the
Graduate Faculty in Partial Fulfillment of
The Requirements for the Degree of
DOCTOR OF PHILOSOPHY

Major Subject: Analytical Chemistry

Approved:

Signature was redacted for privacy.
In Charge of Major Work

Signature was redacted for privacy.
Head of Major Department

Signature was redacted for privacy.
Dean of Graduate College

Iowa State University
Of Science and Technology
Ames, Iowa

1963

TABLE OF CONTENTS

INTRODUCTION

In recent years the analytical spectroscopist has made increasing use of electrical discharges in environments other than air to vaporize samples and excite their emission spectra because distinctive benefits can be gained by using these environments. His earliest motivation in this direction was to eliminate certain interfering molecular band systems. It is well known that when a carbon arc is employed in an atmosphere containing nitrogen, the molecule CN is formed. When excited in the arc column, this molecule emits intense band spectra in the near ultraviolet region of the spectrum. If the simple expedient of conducting a carbon arc in a rare gas, such as helium or argon, is employed, these band spectra are not encountered and analytically useful spectral lines which were completely obscured previously may be exploited.

The atmosphere surrounding the discharge contributes the principal components to the arc plasma and thus plays the dominant role in determining the nature of the electrode vaporization and excitation processes. How these various processes are interrelated under changing environmental conditions has been the subject of considerable experimentation and much discussion, but the exact nature of most of these processes is still not well defined. Some significant generalizations can be drawn, however, illustrating the advantages

of rare gas atmospheres over air, from the work of previous investigators (1, 3, 5, 15, 19, 37, 40, 52-55).

1. The over-all background is reduced.

2. Lower anode temperatures are observed which result in decreased volatilization rates of the more volatile elements and, subsequently, greater efficiency of excitation of atoms liberated into the arc column.

3. Lines of rather high excitation potential may be enhanced in intensity and in some cases lines not observed in air discharges are excited sufficiently to be analytically utilized (oxygen, nitrogen, hydrogen, halogens and sulfur).

Some of these intensity enhancements may undoubtedly be attributed to excitation by collisions of the second kind with metastable excited argon and helium atoms. However, in the majority of the cases it appears that the excitation is due to inelastic collisions with electrons having a distribution of energies higher than that attained in air discharges.

A comparison of the present concepts of excitation in d.c. arc discharges in air and rare gas atmospheres does much to clarify the observed differences in line emission of these discharges. It is generally accepted that in air discharges the electrons and gaseous particles are in thermal equilibrium. This means that the kinetic energy of the electrons and the various energy modes of the gas particles may all be represented by a Maxwell-Boltzmann distribution with a

specified temperature. The excitation of the various electronic states of the gas particles is dominated by inelastic collisions with the electrons. However, the distribution of energies of the various species is controlled by the major process requiring the least expenditure of energy in the discharge. In air atmospheres this process is the dissociation of molecular oxygen, which requires an energy of 5.1 eV. The other two major processes, the dissociation of molecular nitrogen and the ionization of the various species require respectively 9.76 and approximately 12 eV.

The principal mechanism involved in this dissociation process is that of atom-molecule rather than electron-molecule collisions due to the very low energy transfer during elastic collisions with electrons. This then would tend to restrict the energy distribution so that very few atoms would have energies much greater than 5.1 eV. Since the electrons are in thermal equilibrium with the atoms, their energies would also be restricted in the same manner. In argon or helium discharges, however, the limiting process is the ionization of the argon or helium atoms with energy requirements of 15.75 and 24.5 eV respectively. Therefore in arc discharges in rare gas atmospheres, the energy distribution of the electrons, which again may be expected to dominate the excitation via inelastic collisions, will be shifted to values considerably higher than those attained in air. This is illustrated

qualitatively in Figure 1. If, indeed, these energies may still be described by a Maxwell-Boltzmann distribution, then higher temperatures must prevail in argon and helium discharges than those prevailing in air discharges.

Spectroscopic temperature measurements are generally based on the following equation for the intensity of a spectral line (17, 21, 23, 30, 33):

$$I_{nm} = (CNg_n A_{nm} \nu_{nm}/Q) \exp(-E_n/kT) \quad (1)$$

where

- C = constant depending on geometry of source
- N = total number density of the emitting species
- g_n = statistical weight of the initial level of the transition
- A_{nm} = Einstein transition probability
- ν_{nm} = energy of the transition
- Q = partition function
- E_n = energy of the initial state
- k = Boltzmann's constant
- T = temperature (°K)

In theory if all of the factors except the temperature on the right side of the equation are known, a measurement of the absolute intensity of the spectral line would give the temperature of the source. In practice this is seldom done

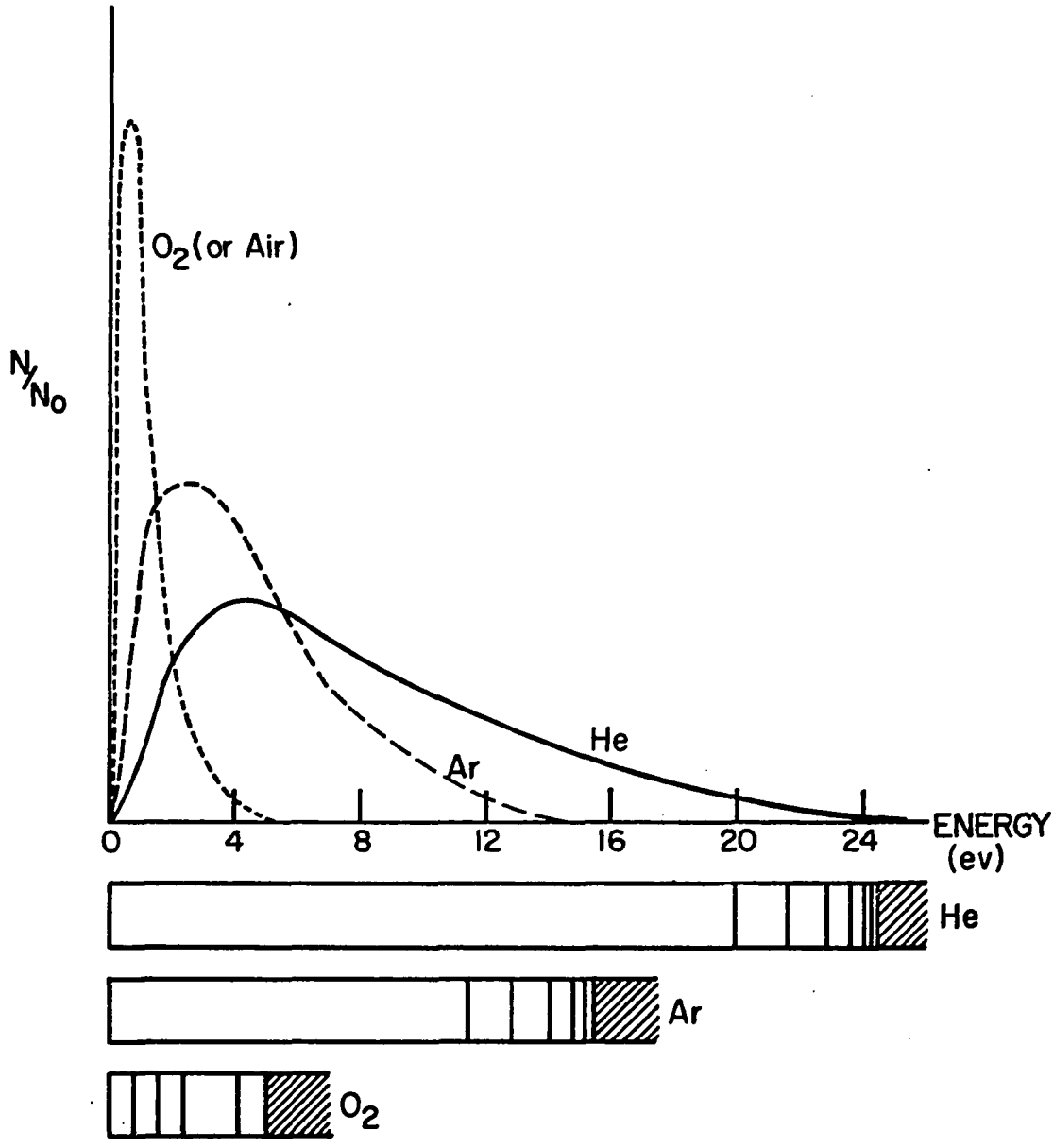

Figure 1. Electron energy distribution curves

because some factor such as the number density of the emitting species or the Einstein transition probability is not known accurately. In addition, absolute intensity measurements are very difficult to perform. Therefore, the usual practice is to measure the relative intensities of several lines of the same species. The factors in the equation dependent only on the species (C, N and Q) then cancel and the temperature can be obtained either from the intensity ratio of two of these lines or from a log plot of the relative intensities of several lines versus their respective energies. These methods have the added advantage that relative transition probabilities are much more readily obtained than their absolute counterparts.

Several restrictions and precautions must be noted in carrying out these procedures. Equation 1 assumes that no self absorption is exhibited by the spectral lines. This can generally be insured by using low concentrations of the thermometric species in the discharge and avoiding the use of resonance lines. Equation 1 also assumes that the source is in thermodynamic equilibrium described by the temperature T. The arc usually is pictured as being in local thermodynamic equilibrium which means that each infinitesimal volume element is in thermodynamic equilibrium with a steady state exchange of energy between adjacent volume elements. This steady state energy exchange generates a radial

distribution of temperatures ranging from slightly above room temperature at the extreme periphery to many thousands of degrees at the central axis of the arc column. The axial temperature gradient is assumed to be zero except in the immediate vicinity of the electrodes.

These radial temperature distributions in the arc column were ignored in most early temperature measurements with the result that, at best, the temperatures obtained were somewhat of an average of the temperatures prevailing in the portion of the source viewed by the spectrograph. The main reason for ignoring these temperature distributions was undoubtedly the experimental difficulty associated with the determination of their exact form. However, in recent years a method has been developed for determining the radial temperature profiles of high current arcs and plasma jets (9, 22, 26-28, 31, 32, 34, 35, 39, 43, 45, 48, 57). Referring to Equation 1, it will be noted that the exponential term and also the partition function will increase with increasing temperature. The concentration factor, N, will decrease with increasing temperature because of several factors, such as dissociation, ionization and the ideal gas law decrease of gas density at constant pressure. Therefore, every spectral line will exhibit a maximum in its intensity versus temperature profile, I(T), at some temperature. The temperature at which this maximum occurs in the intensity profile can be calculated

if the transition probability and the concentration of the species as a function of temperature and pressure are known. If the intensity of this spectral line is then measured as a function of the radius of the discharge and exhibits a maximum, the temperature at this radius must be equal to the calculated temperature.

In practice the experimental measurement of the intensity as a function of the radial distance from the axis, I(r), is rather complex. The following description presumes cylindrical symmetry of the discharge with respect to the axis and negligible self absorption. The discharge can then be represented as shown in Figure 2 by n concentric zones, each zone being characterized by a particular temperature. A series of measurements of the intensity perpendicular to the x-axis, I(x), can then be made by moving the source in the x direction. The measurements of I(x) can also be accomplished by rotating the image of the discharge by 90° with a system of mirrors such that the slit of the spectrograph is perpendicular to the arc column. Short segments of the photographic image of the spectral line may then be microphotometered to obtain a number of values of I(x) across the diameter of the discharge.

Because of the variation of the depth of the arc column as a function of position along its diameter, it is necessary to convert the values of I(x) to values of I(r). By the use

of cylindrical coordinates, as illustrated in Figure 3, the following relationship between I(x) and I(r) can be obtained.

$$I(x) = 2\int_{x}^{R} I(r)rdr/\sqrt{r^2-x^2} \tag{2}$$

This is the well known Abel integral equation which inverts to the form

$$I(r) = -\frac{1}{\pi}\int_{r}^{R} I'(x)dx/\sqrt{x^2-r^2} \tag{3}$$

where the prime denotes differentiation with respect to x and R is the total radius of the arc column. Equation 3 must be solved either numerically or graphically because an analytical expression for I(x) is generally not known.

A direct knowledge of the value of the transition probability may be circumvented in the calculation of I(T) by normalizing the curve such that the maximum point is set equal to unity. This normalization method may also be applied to I(r), thus allowing the measurement of relative rather than absolute intensities.

The radial temperature distribution of the discharge can be obtained by equating I(T) and I(r) if one value of T(r) is known independently. This independent value is obtained by specifying the temperature at the maximum point in I(T) to correspond to the radius at the maximum point in I(r). The

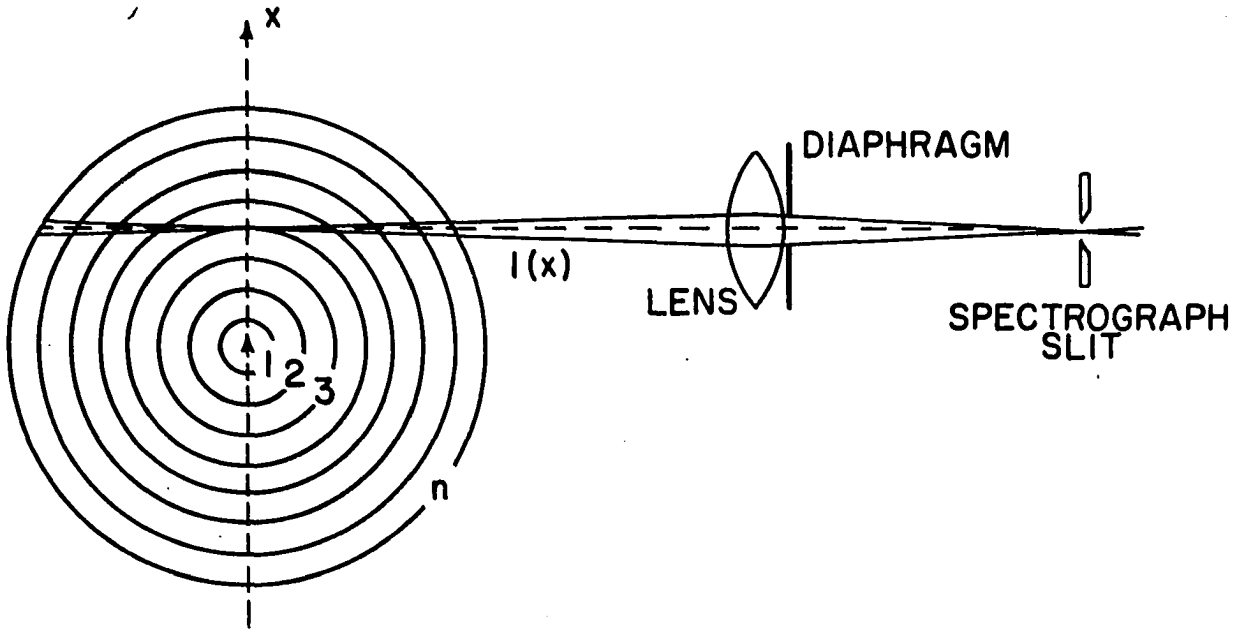

Figure 2. Optical arrangement for measuring I(x)

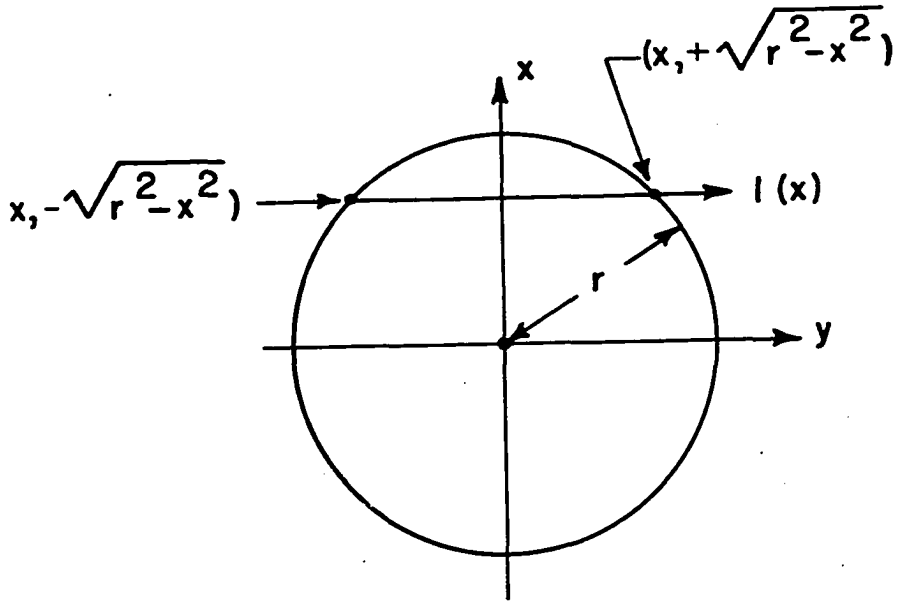

Figure 3. Schematic diagram identifying the coordinates used in the analysis of an axially symmetric arc

main disadvantage of this method for determining the radial temperature distribution is that the maxima in the I(T) and I(r) curves may be quite broad and therefore it is difficult to determine accurately the initial value of T(r).

This method has been applied to spatially stable high temperature discharges. In general, the temperatures at the axes of these discharges have ranged from 15000° to 35000°K, and ionic species have been employed for the measurements. Unfortunately, the low current arcs of interest to the analytical spectroscopist exhibit spatial instability to such a degree that it is impossible to obtain accurately the intensity measurements required for the above method.

The literature contains very little concerning actual temperature measurements on low current arc discharges in rare gases. Marzuvanov (38) studied d.c. arc discharges between graphite electrodes in flowing atmospheres of argon and helium. The electrodes were spaced approximately 5 mm apart and a current of 10 amperes was employed. The anode cup was filled with powdered graphite containing 1% copper. Copper lines were employed for the temperature measurements and gave values of 6700 to 6800°K in the peripheral zones of the arc column in helium. In air these same lines gave a temperature of 5600°K at the axis of the discharge. Argon gave results similar to those obtained in helium. Marzuvanov noted that the neutral atom copper lines at 5105.54 and 5153.23Å, which

he employed for these measurements, disappeared in the core of the discharge. This was presumably due to almost total ionization of the copper. He attempted to obtain some insight of the radial temperature distribution by applying the method described above. In order to minimize the undesirable effects created by the wandering of the arc, 40-50 exposures were made of 0.01 second duration. Even then only a small number of these exposures could be employed. From these measurements he concluded that the temperature 0.5 mm from the axis was 7200°K and that the temperature at the axis was significantly higher than this value. However, since the copper lines essentially disappeared at the axis, reliable measurements could not be made at radial distances shorter than 0.5 mm. The data in his paper were sketchy and no mention was made of the values employed for the transition probabilities of the copper lines.

Two other papers (14, 51) pose the basic question of whether the assumption of the existence of thermal equilibrium in rare gas arc discharges at atmospheric pressure is really valid. The basic equation for the intensity of a spectral line is

$$I_{nm} = CN_n A_{nm} h\nu_{nm} \qquad (4)$$

where C is a constant dependent upon the geometry of the

source and N_n is the number density of the emitting species in the initial state of the transition. This equation is valid regardless of whether thermal equilibrium exists. The assumption of thermal equilibrium implies the existence of a Maxwellian distribution of the energies of the particles as shown in the following equation

$$N_n/N_o = (g_n/g_o) \exp(-E_n/kT) \quad (5)$$

where N_o is the number density of particles in the ground state. This may also be expressed as follows

$$\log(N_o/g_o) - \log(N_n/g_n) = 5040\ E_n/T \quad (6)$$

where E_n is in units of electron volts. A plot of log (N_n/g_n) vs. E_n should result in a straight line with a slope of -5040T and intercept of $\log(N_o/g_o)$ if thermal equilibrium exists. Egorov et al. (14) determined the absolute populations, N_n, of energy levels of helium, hydrogen and neon atoms in arc discharges in argon and helium at atmospheric pressure by measuring the absolute intensities of selected spectral lines of these three elements. With knowledge of the absolute intensity, I_{nm}, the value of N_n could then be calculated from Equation 4. This operation presumed an accurate knowledge of transition probabilities and certain geometrical factors re-

lated to the entrance optics of their spectrographic illumination system. No mention was made in this paper of either factor. The values of $\log(N_n/g_n)$ were then plotted vs. E and are shown in Figure 4. Extrapolation of the straight lines obtained gave unrealistically high values of $\log(N_o/g_o)$ corresponding to pressures of millions of atmospheres in the discharges. Rough calculations of the actual values of $\log(N_o/g_o)$ were made and the slope of the dashed straight line connecting these values with the center of the experimental values of $\log(N_n/g_n)$ gave absolute temperatures of approximately 11000°K. The slopes of the solid straight lines formed by the relative values of $\log(N_n/g_n)$ vs. E gave relative temperatures of approximately 3500°K. In addition, measurements of relative intensities of the vibrational bands of CN gave temperatures of 3000 to 4000°K.

The radial distribution of line intensities, I(r), was also measured and indicated emission from low energy diatomic molecules and high energy atoms simultaneously from the central regions of the discharges. The discrepancy of a factor of 3 to 4 between the absolute and relative population temperatures plus the coexistence of thermally stable and unstable species in the same regions of the discharge were taken to indicate the absence of thermal equilibrium.

Sobolev et al. (51) extended this work by vaporizing large quantities of barium, copper and lithium into arc

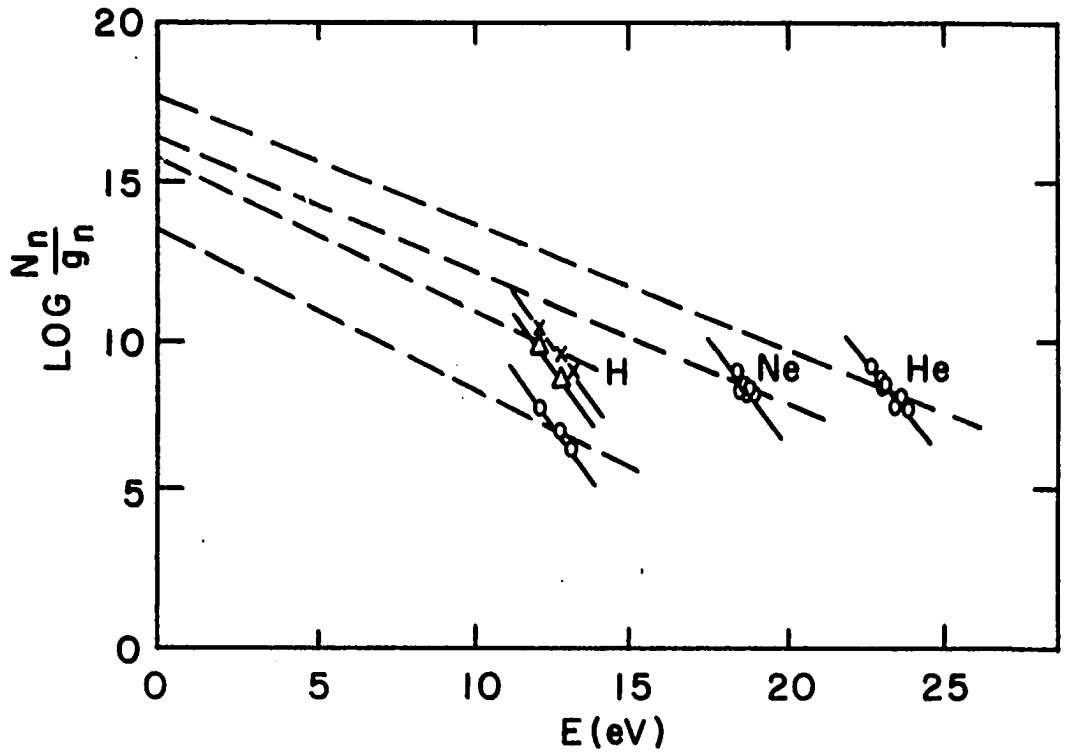

Figure 4. Population of excited levels of atoms of H, He and Ne (14)

discharges in argon and helium. Relative population temperatures of 6000 to 7000°K were obtained from Ba II and Cu I lines at the axis and temperatures of 3000 to 4000 °K were obtained with Ba I and Li I lines in the peripheral regions of the arc column. The emission of hydrogen, helium and argon spectra was almost completely suppressed by the introduction of these metallic impurities. It was concluded from these results that thermal equilibrium was approached with the addition of large amounts of metallic vapors into rare gas arc discharges.

The same criticisms which applied to Marzuvanov's paper (38) also apply here. The data are sketchy and no transition probabilities are given. In addition, absolute measurements are made without any indication of the methods employed.

Sobolev et al. (51) refer to papers by Druyvesteyn and de Groot (12) and Ornstein and Brinkman (44) as supporting their conclusions that equilibrium may not exist in these discharges. Both of these papers, written approximately thirty years ago, are theoretical rather than experimental in nature and unfortunately their theories suffer in that they ascribe far too little significance to the role played by electrons in excitation processes.

The purpose of this thesis is to explore another technique for obtaining data which may provide further insight into the nature of arc discharges in rare gas atmospheres and

hopefully to provide more definitive information on the excitation temperatures. In order to clearly define how our experimental approach will differ from prior methods, let us first consider the problem of radial temperature distribution. This not only requires a consideration of the actual radial temperature distribution but also the effect of the temperature variation on the radial distribution of concentration of the emitting thermometric species. As noted above, others have employed the technique of observing line intensity profiles emitted along the projected diameter of the arc plasma and have reduced these observations to intensities emanating from radial layers of constant temperature, using a standard inversion of the Abel integral. These techniques have been employed primarily for high current arcs (on the order of 200-400 amperes) possessing a high degree of spatial stability. Unfortunately, the analytical spectroscopist is primarily interested in lower current arcs (5-30 amperes), which exhibit considerable wandering at atmospheric pressure. This wandering destroys to a large degree the spatial resolution required by the aforementioned methods.

To circumvent basic uncertainties arising from this experimental deficiency, the experimental approach developed in this thesis is based on the observation of both molecular and atomic radiation emitted by the entire horizontal cross section of the arc column, exclusive of the immediate vicinities

of the electrodes. Under these conditions the observed spectral intensities will then reflect the integrated intensities from all zones of varying temperature.

It is possible to calculate the theoretical integrated intensities or intensity ratios as a function of the maximum temperature of the discharge if the transition probabilities and the radial temperature and concentration distributions are known. The concentrations of the emitting species as a function of temperature are readily calculable by the methods of statistical thermodynamics and the solution of equations describing simultaneous equilibria. Accurate transition probabilities are available through simple calculations, if the rotational spectra of diatomic molecules are employed. Reasonably accurate relative values for some spectral lines of neutral atoms are also available in the literature. The radial temperature distribution, as noted above, is not readily determinable and, for the purposes of this work, several different forms will be assumed and the results of their application will be critically analyzed. All measurements and calculations of spectral intensities will be made on a relative basis in order to avoid the inherent difficulties and inaccuracies of absolute measurements. Comparison of the observed relative spectral intensities with the calculated values as a function of the maximum temperature should then give us an insight of the temperature existing

at the axis of the arc column. In this thesis several different thermometric species of widely differing character will be employed to insure adequate cross-checking of the temperatures obtained and to verify the assumption of the existence of thermal equilibrium.

The thermodynamic calculations of the concentrations of the thermometric species and the requirement of a knowledge of accurate transition probabilities are greatly facilitated if a system employing simple chemical equilibria involving diatomic molecules is selected. To fulfill these criteria, the discharges studied in this work will be d.c. carbon arcs at atmospheric pressure in helium or argon containing small amounts of nitrogen. Thus, three chemical reactions must be considered in the calculations.

$$CN \rightleftharpoons C + N$$

$$C_2 \rightleftharpoons 2C$$

$$N_2 \rightleftharpoons 2N$$

The equilibrium constants of these three reactions will be calculated as a function of temperature up to 15000°K. A system of simultaneous equations will then be solved to obtain the concentrations of various species as a function of temperature.

Since the ultraviolet rotational spectrum of CN is well documented, a large portion of the intensity measurements

will be devoted to this species. In addition, measurements will be made on the intensities of selected nitrogen and argon atomic lines.

The assumption of the existence of local thermodynamic equilibrium is made in the calculations and the validity of this assumption is discussed in relation to the results obtained in this work.

EXPERIMENTAL

The study of rare gas discharges necessitates the use of an airtight discharge chamber. The chamber used in this study is illustrated in Figure 5. There is a single fixed upper electrode assembly and a rotating stage type of lower electrode assembly, capable of accepting nine electrodes. These may be moved into position under the fixed electrode by external use of a small permanent magnet. The chamber may be evacuated to pressures in the order of 10^{-5} Torr by means of an oil diffusion pump and a mechanical forepump.

Suitable gas manifolds and valves are attached to the chamber so that two gases may be added to the chamber in any proportion. Two pressure gauges, a Bourdan type and a mercury manometer, are used for determining the amount of gas admitted to the chamber.

The spectrograph used in conjunction with this arcing chamber was a Jarrell-Ash, Mark IV Ebert mount, with a 15000 lines per inch plane grating blazed for maximum intensity at 13000Å first order. The external optical system consisted of a spherical condensing lens, a mirror, a diaphragm and two crossed cylindrical lenses. This is illustrated in Figure 6. The spherical lens focussed the arc on the diaphragm with a twofold magnification. The electrode images were masked at the diaphragm. The radiation from the center two thirds of

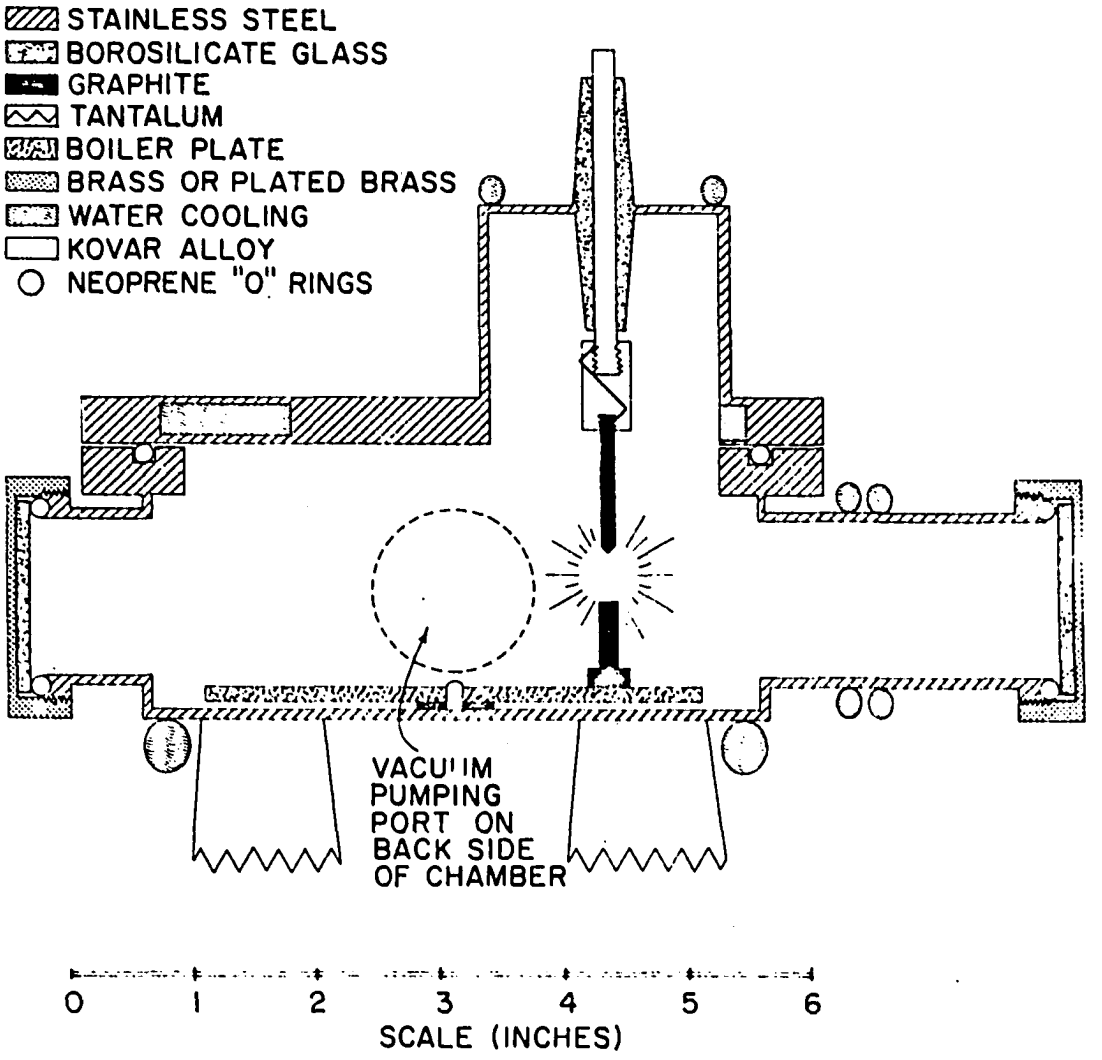

Figure 5. Discharge chamber

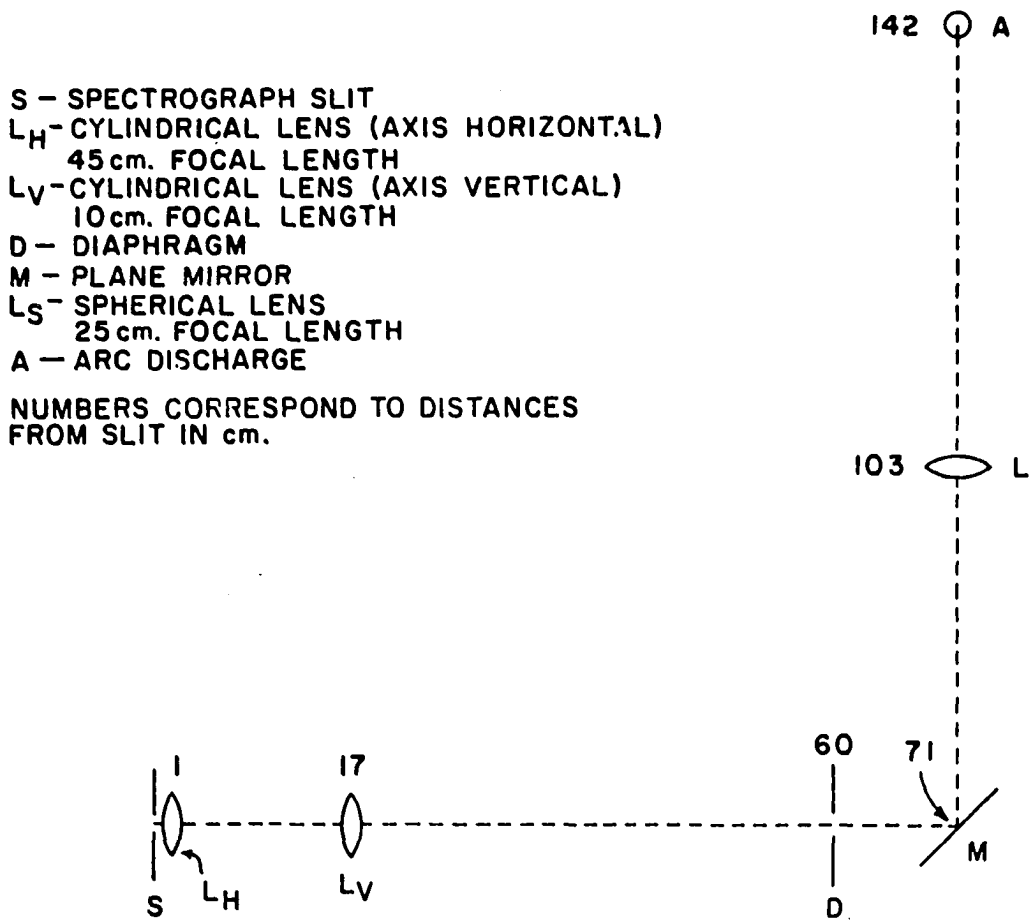

Figure 6. External optical system

the discharge was imaged behind the collimating mirror by the combination of the two cylindrical lenses. This arrangement allowed the viewing of the entire discharge diameter by the spectrograph. A rotating step sector with a uniform intensity ratio between adjacent steps of 1.585 was placed immediately in front of the spectrograph slit; spectrograms obtained with this step sector allowed calibration of the photographic plate.

The source unit employed was a National Spectrographic Laboratories "Spec-Power" capable of maintaining a 35 ampere d.c. arc discharge between graphite electrodes spaced 6 mm apart in air. In argon and helium atmospheres the maximum currents attainable between graphite electrodes with a gap spacing of 6 mm were 30 amperes and 28 amperes, respectively.

The cathode of the discharge was a 1/8 inch diameter graphite rod and the anodes were graphite rods of 5/16 inch diameter at the base and 3/16 inch diameter over the upper half of their length. The smaller diameter of the anodes at the discharge end tended to reduce considerably the wandering of the anode spot and thus helped to stabilize the cylindrical symmetry of the discharges.

The tank helium, argon and nitrogen used in these experiments was sufficiently pure to be used directly without further purification. The electrodes were individually degassed prior to a run by means of a 30 second arc discharge

in argon or helium followed by evacuation of the chamber. A 3 minute arc discharge to a 5/16 inch diameter block electrode heated the chamber walls sufficiently to remove any adsorbed gases. In addition, each electrode was given another 30 second degassing just prior to making an exposure with it.

The majority of the exposures were obtained from discharges in atmospheres of argon or helium which contained either 0.05 or 1.0 volume per cent of nitrogen. The lower concentration of nitrogen was obtained through the use of commercial gas mixtures containing 0.05% nitrogen in argon and helium. The higher concentration was attained by addition of 1.0 volume per cent of nitrogen to the evacuated chamber and subsequent addition of argon or helium. In all cases a total gas pressure of one atmosphere at 300°K was employed.

A 6 mm arc gap was employed for all discharges. A current of 28 amperes was used in argon atmospheres and 26 amperes in helium atmospheres.

The exposures of the CN $^2\Sigma$-$^2\Sigma$ bands were made in the fourth order using Kodak III-O photographic plates. A Pyrex glass filter was employed to remove any higher order interferences and the wavelength sensitivity of the emulsion removed the possibility of any lower order interferences.

The reciprocal linear dispersion on the photographic plate was 1.1Å per mm in the fourth order. It was found that

the optimum slit width for the spectrograph was between 25 and 10 microns. Most of the data were obtained with a 25 micron slit width because the shorter exposure times required overrode the slightly better resolution obtained with the 10 micron slit width.

It was necessary to prefog the plate prior to making an exposure in order to obtain a measurable background level. This was accomplished by a 30 second exposure with a 40 watt tungsten lamp mounted on the optical bench immediately behind the chamber. These prefoggings were also sectored if the arc exposure superimposed upon it was to be sectored. A sectored exposure of the iron spectrum was included on every plate for calibration purposes.

The exposure time of the arc discharges was variable, falling in the range of 1-5 minutes, depending on the slit width, the supporting atmosphere and the concentration of nitrogen present.

The photographic plates were developed for 3 minutes in Kodak D-19 and fixed for 10 minutes in Kodak Acid Fixer. They were then washed for 40 minutes in running water and dried for 5 minutes over a hot air blower.

The selection of line pairs to be used for temperature measurements was dictated by their ability to fulfill the four following conditions.

1. The transition probabilities must be readily

calculable or available in the literature.

2. A large difference in energy of the initial states of the two lines is desirable in order to obtain as large a change of intensity ratio with change in temperature as possible.

3. The lines should be in close wavelength proximity to avoid errors due to sensitivity variation of the photographic emulsion with change of wavelength.

4. Freedom of interference from other spectral lines is necessary.

Two rotational lines in the 0 - 0 vibrational band of the $^2\Sigma$-$^2\Sigma$ electronic transition met the above criteria. These lines were (1) an R branch line with its lower level rotational quantum number, J", equal to 14 and (2) a P branch line with J" equal to 56. These lines will hereafter be referred to as R_{14} and P_{56}. Figure 7 indicates their location in the band system. Atomic argon lines of wavelength 4259.36Å and 4272.16Å and atomic nitrogen lines of wavelength 8680.24Å and 8629.24Å were also selected. No helium or carbon line pairs could be found which fulfilled the required conditions.

The argon spectra were photographed using the same plates and conditions employed for the CN spectra. The nitrogen spectra were photographed in the first order with Kodak I-N plates. A filter with a sharp cutoff below 6500Å was employed to eliminate higher orders. The only difference

Figure 7. Location of the P_{56} and R_{14} lines in the 0 - 0 band of the $^2\Sigma$ - $^2\Sigma$ CN transition

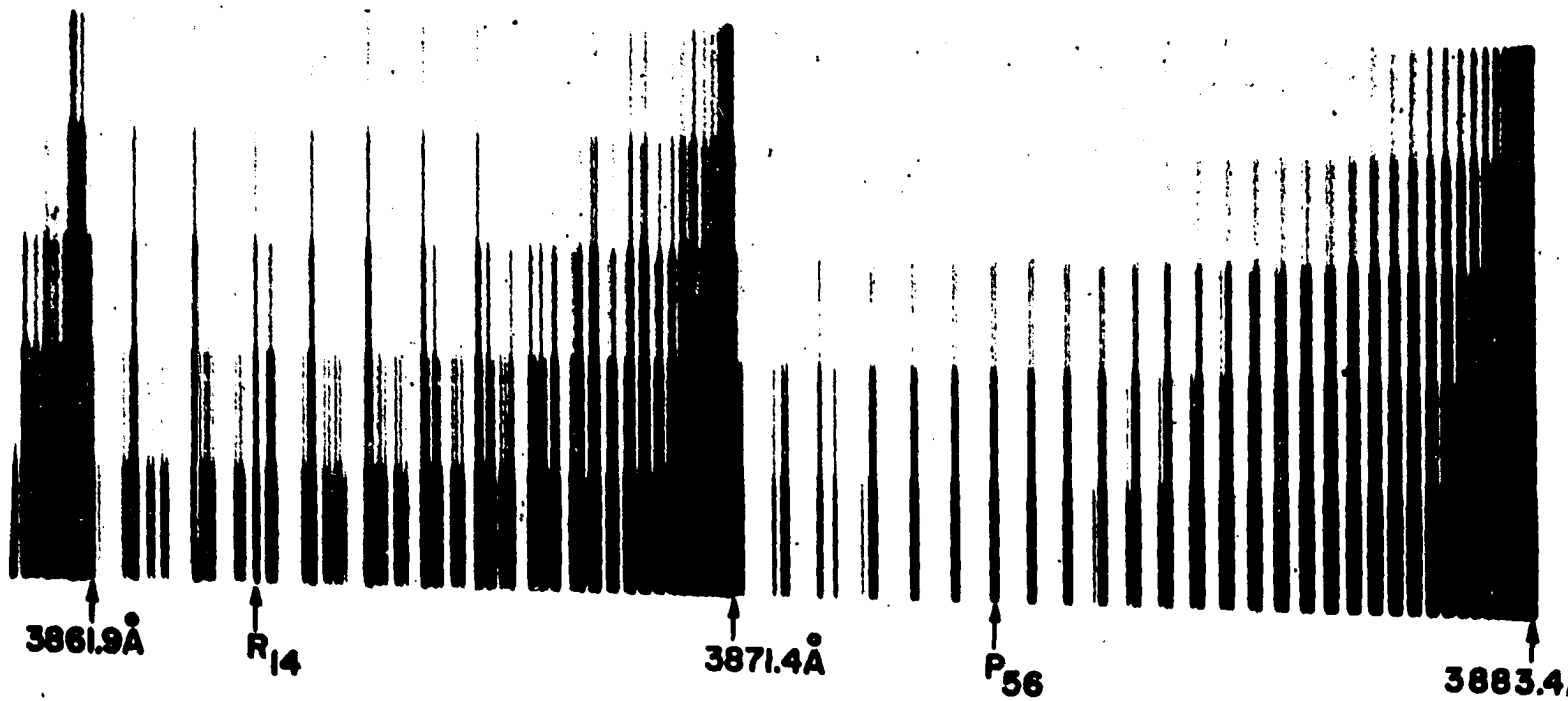
3861.9Å
R14
3871.4Å
P56
3883.4Å

in processing the I-N plates was the use of a 4 minute developing period as contrasted to a 3 minute developing period for the III-O plates.

The CN lines are in reality doublets, as will be explained in the next section. The doublet spacing increases with increasing value of J and this posed a problem because the P_{56} doublet components were partially resolved whereas the R_{14} components were completely unresolved. Therefore the peak intensities could not be employed for measurement but rather the area intensity ratios had to be determined. Fortunately, a National Spectrographic Laboratories, Inc. recording microphotometer was available to solve this problem.

The line profiles in per cent transmission were obtained using an 8 micron microphotometer slit width, a 0.17 mm per minute plate carriage scan rate and a 3 inch per minute recorder chart speed. These line profiles were then converted to relative intensity profiles by taking the per cent transmission values at 1/8 inch intervals and converting them to relative intensity values by means of the plate calibration curve. The relative intensity values were plotted on linear graph paper and the area above the background level determined with a planimeter. The intensity ratio of P_{56}/R_{14} was then determined by division of the relative areas.

A comparison of the relative intensity line profiles of

the P_{56} and R_{14} lines is shown in Figure 8.

The area intensity ratio was found to be higher than the peak intensity ratio by an average factor of 1.689. All subsequent measurements were made of the peak intensity ratios, which were then multiplied by 1.689 to obtain the area intensity ratios. This greatly reduced the amount of time required to make these measurements while still maintaining an acceptable degree of accuracy.

The argon lines exhibited a marked asymmetry, in the form of a degradation toward the red. Therefore it was necessary to measure the area intensity ratios by the same techniques which were employed for the CN lines. It was determined that a multiplicative factor of 1.185 could be used to convert the peak intensity ratio of Ar 4259.36Å / Ar 4272.16Å to the area intensity ratio.

The nitrogen lines exhibited no asymmetry and the area and peak intensity ratios of N 8629.24Å / N 8680.24Å were identical.

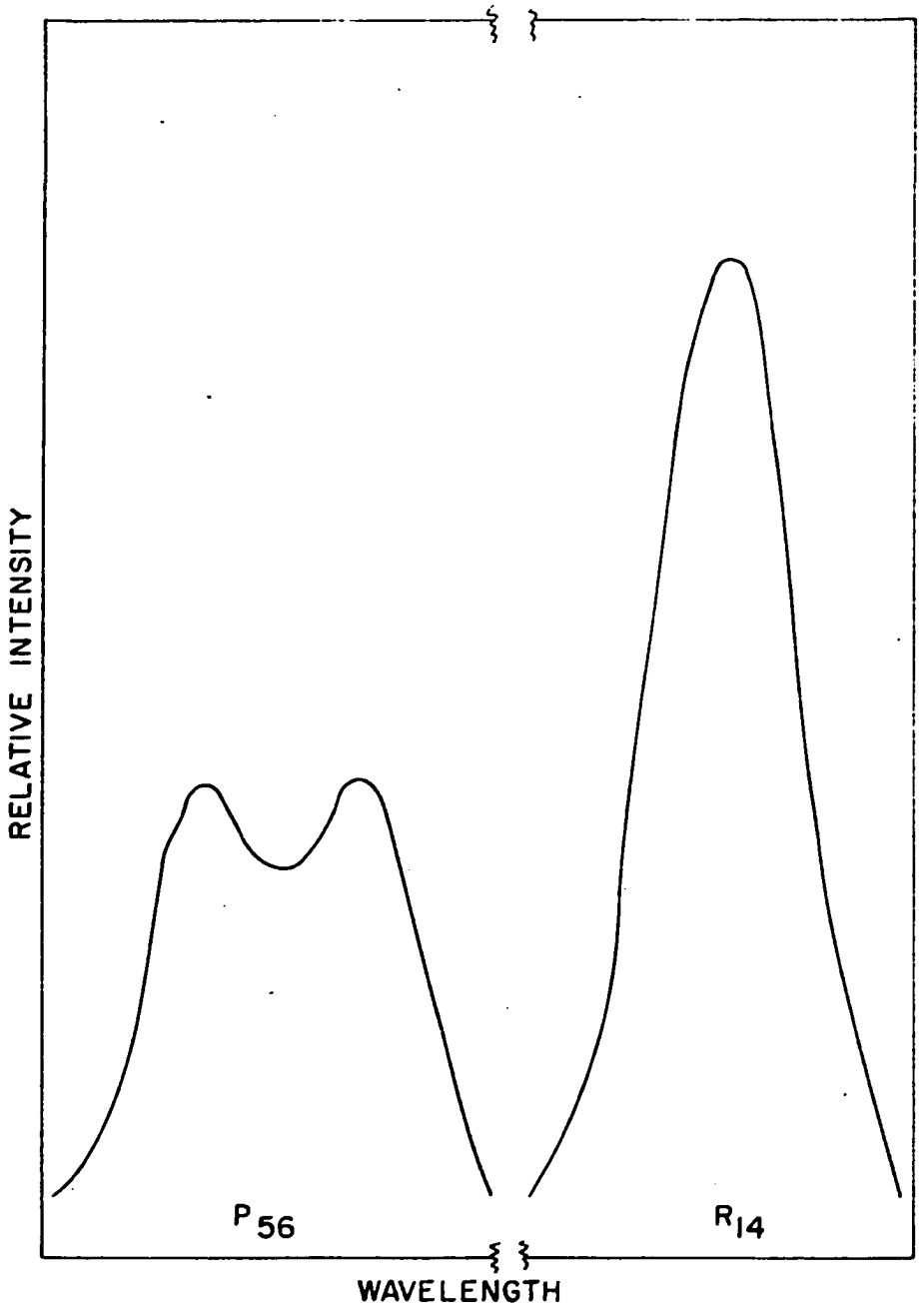

Figure 8. Relative intensity profiles of the P_{56} and R_{14} CN lines

THEORETICAL CALCULATIONS

Equilibrium Constants

If the reaction

$$AB \rightleftharpoons A + B$$

is considered, according to statistical thermodynamics, the equilibrium constant at temperature T is given by

$$K = [(Q_A/N)(Q_B/N) / (Q_{AB}/N)] \exp(-E^{\circ}_{AB}/RT) \quad (7)$$

where Q is the total partition function of the species in subscript, E°_{AB} is the dissociation energy of AB, N is Avogadro's number, R is the gas constant and T is the absolute temperature (4, 56).

The partition function is defined by the equation

$$Q = \sum_{i=1}^{\infty} g_i \exp(-E_i/kT) \quad (8)$$

where E_i and g_i are, respectively, the energy and degeneracy of state i, and k is Boltzmann's constant. The total energy is composed of the sum of the translational, electronic, vibrational and rotational energies. Of these, only the translational form is non-quantized and may be considered entirely independently from the other three. The vibrational

and the rotational energies are intertwined and must be considered together. They may be combined with the electronic energy in the following manner to give the internal partition function

$$Q_{int.} = \sum_{i=1}^{\infty} Q_{i\ el.} \cdot Q_{i\ vib.-rot.} \tag{9}$$

The internal partition function is then multiplied by the translational partition function to yield the total partition function

$$Q = Q_{trans.} \cdot Q_{int.} \tag{10}$$

The translational partition function for any species is given by the equation

$$Q_{trans.} = (V/h^3)(2\pi mkT)^{3/2} \tag{11}$$

where V is the volume of the system, h is Planck's constant and m is the mass of the species. Assuming that the ideal gas law will be valid, RT/P may be substituted for V. Also, the molecular weight, M, divided by Avogadro's number, N, may be substituted for m. The final equation for calculation of the translational partition function is then

$$Q_{trans.} = (2\pi Mk/Nh^2)^{3/2} (R/P)(T)^{5/2} \quad (12)$$

The vibrational-rotational partition function is equal to unity for all monatomic species. For diatomic molecules this partition function is given (47) by

$$Q_{vib.-rot.} = (1/\sigma y(1-e^{-u})) [1+(2\beta/y)+(\delta/e^{u}-1) + (2x_e u/(e^{u}-1)^2)+(y/3)+(y^2/15)] \quad (13)$$

where

$u = hc\omega_o/kT$

$\omega_o = \omega_e - 2\omega_e x_e$

$y = hcB_o/kT$

$B_o = B_e - \alpha/2$

$\beta = D/B_o$

$\delta = \alpha/B_o$

$D = 4B_e^3/\omega_e^2$

σ = 1 for heteronuclear, 2 for homonuclear molecules

This equation takes into account the anharmonicity of the vibrations and the non-rigidity and centrifugal stretching of the rotations of the molecule.

The internal partition function is obtained from the equation

$$Q_{int.} = \sum_{i=1}^{\infty} g_i \exp(-E_i/kT) \cdot Q_{i\ vib.-rot.} \qquad (14)$$

where g_i and E_i are, respectively, the degeneracy and energy of the electronic state i. The degeneracy for the electronic energy levels of a monatomic species is given by 2J + 1. For the case of diatomic molecules

$$g_{el.} = 1 \text{ for } {}^1\Sigma \text{ states}$$

$$= 2 \text{ for } {}^2\Sigma,\ {}^1\pi,\ {}^2\pi_{1/2},\ {}^2\pi_{3/2},\ {}^3\pi_0,\ {}^3\pi_1,\ {}^3\pi_2 \text{ and } {}^1\Delta \text{ states}$$

$$= 3 \text{ for } {}^3\Sigma \text{ states}$$

$$= 4 \text{ for } {}^2\pi\ ({}^2\pi_{1/2 + 3/2})$$

$$= 6 \text{ for } {}^3\pi\ ({}^3\pi_{0 + 1 + 2})$$

The physical constants employed in these calculations were obtained from Dumond and Cohen (13) and are shown in Table 1. The electronic, vibrational and rotational constants for the diatomic molecules are listed in Table 2.

The internal partition functions of the monatomic species as well as the vibrational-rotational partition functions of the diatomic molecules were calculated with the aid of an IBM 650 digital computer. The degeneracies and energies of

Table 1. Physical constants

k	1.38044×10^{-16} erg/°K
h	6.62517×10^{-27} erg sec
c	2.997930×10^{10} cm/sec
N	6.02486×10^{23} atoms/mole
R	82.08200 cm^3 atm./mole °K
ln 10	2.302585
π	3.141593

the various levels of the nitrogen and carbon atoms were obtained from the compilation by Moore (41).

The internal partition functions for the species N_2, C_2, CN, C and N are listed in Table 3 and the total partition functions are listed in Table 4. In these tables and several of the following ones the subheadings A and B are employed. These subheadings correspond to the form $A \times 10^B$ for the presentation of the data.

The equilibrium constants for the dissociation reactions of N_2, C_2 and CN were calculated using the dissociation energies listed in Table 5. The K_p's (atmospheres) were converted to K_c's (moles/liter) through division by RT. The K_c's for the three reactions are given in Table 6.

Table 2. Molecular constants

Molecule	State	T_e	ω_e	$\omega_e x_e$	B_e	α_e
CN (20)	B $^2\Sigma^+$	25951.8	2164.13	20.25	1.9701	0.02215
	A $^2\pi_i$	9241.66	1814.43	12.883	1.7165	0.01746
	X $^2\Sigma^+$	0	2068.705	13.144	1.8996	0.01735
N_2 (42)	a $^1\pi_g$	68953	1693.70	13.83	1.6090	0.0183
	B $^3\pi_g$	59314	1734.11	14.47	1.6288	0.0184
	A $^3\Sigma_u^+$	49757	1460.37	13.89	1.433	0.013
	X $^1\Sigma_g^+$	0	2358.07	14.19	1.990	0.017
C_2 (2,6)	d $^1\Sigma_u^+$	43240.23	1829.57	13.97	1.8334	0.0204
	B $^3\pi_g$	39470.4	1106.56	39.26	1.1922	0.0242
	c $^1\pi_g$	34261.9	1809.1	15.81	1.7334	0.0180
	A $^3\pi_g$	18696.3	1788.22	16.44	1.7527	0.01608
	$^3\Sigma_u^+$	14300				
	b $^1\pi_u$	8268.33	1608.35	12.07	1.61634	0.0168
	$^3\Sigma_g^-$	6243.5	1470.45	11.19	1.4985	0.01634
	X $^3\pi_u$	610	1641.35	11.67	1.6326	0.01683
	a $^1\Sigma_g^+$	0	1854.71	13.34	1.81984	0.01765

Table 3. Internal partition functions

	CN		N_2		C_2		C		N	
T	A	B	A	B	A	B	A	B	A	B
250	1.8456	2	4.3839	1	5.7802	1	7.6224	0	4.0000	0
500	3.6974		8.7663		2.0915	2	8.2734		4.0000	
750	5.6436		1.3285	2	4.6301		8.5068		4.0000	
1000	7.7934		1.8154		8.0261		8.6267		4.0000	
1250	1.0210	3	2.3524		1.2244	3	8.6998		4.0000	
1500	1.2924		2.9478		1.7294		8.7491		4.0000	
1750	1.5961		3.6056		2.3208		8.7853		4.0000	
2000	1.9343		4.3282		3.0032		8.8140		4.0000	
2250	2.3100		5.1173		3.7815		8.8389		4.0000	
2500	2.7264		5.9736		4.6612		8.8624		4.0002	
2750	3.1873		6.8981		5.6479		8.8860		4.0004	
3000	3.6973		7.8914		6.7473		8.9109		4.0010	
3250	4.2605		8.9540		7.9650		8.9378		4.0020	
3500	4.8812		1.0086	3	9.3056		8.9671		4.0037	
3750	5.5640		1.1289		1.0777	4	8.9988		4.0064	
4000	6.3249		1.2563		1.2381		9.0330		4.0101	
4250	7.1324		1.3907		1.4126		9.0696		4.0152	
4500	8.0265		1.5324		1.6016		9.1084		4.0220	
4750	8.9985		1.6812		1.8057		9.1493		4.0305	
5000	1.0053	4	1.8373		2.0259		9.1920		4.0411	

Table 3. (Continued)

T	CN A	CN B	N_2 A	N_2 B	C_2 A	C_2 B	C A	C B	N A	N B
5250	1.1192		2.0006		2.2597		9.2364		4.0537	
5500	1.2421		2.1713		2.5135		9.2822		4.0686	
5750	1.3742		2.3494		2.7833		9.3292		4.0858	
6000	1.5158		2.5349		3.0699		9.3773		4.1054	
6250	1.6673		2.7279		3.3754		9.4263		4.1275	
6500	1.8288		2.9285		3.6997		9.4760		4.1519	
6750	2.0008		3.1366		4.0429		9.5264		4.1789	
7000	2.1835		3.3525		4.4058		9.5772		4.2082	
7250	2.3773		3.5761		4.7830		9.6285		4.2399	
7500	2.5821		3.8075		5.1916		9.6802		4.2739	
7750	2.7983		4.0470		5.6183		9.7320		4.3101	
8000	3.0264		4.2947		6.0642		9.7842		4.3485	
8250	3.2664		4.5506		6.5349		9.8365		4.3890	
8500	3.5186		4.8148		7.0286		9.8889		4.4315	
8750	3.7833		5.0878		7.5420		9.9414		4.4760	
9000	4.0605		5.3697		8.0827		9.9941		4.5223	
9250	4.3508		5.6606		8.6500		1.0047	1	4.5703	
9500	4.6541		5.9610		9.2405		1.0100		4.6199	
9750	4.9705		5.2710		9.8557		1.0153		4.6711	
10000	5.3006		6.5911		1.0501	5	1.0206		4.7239	

Table 3. (Continued)

T	CN A	CN B	N_2 A	N_2 B	C_2 A	C_2 B	C A	C B	N A	N B
10250	5.6443		6.9217		1.1168		1.0260		4.7779	
10500	6.0021		7.2632		1.1864		1.0314		4.8334	
10750	6.3739		7.6158		1.2613		1.0368		4.8900	
11000	6.7598		7.9803		1.3348		1.0422		4.9478	
11250	7.1606		8.3570		1.4156		1.0477		5.0067	
11500	7.5757		8.7466		1.4948		1.0533		5.0667	
11750	8.0060		9.1496		1.5819		1.0589		5.1276	
12000	8.4513		9.5667		1.6670		1.0647		5.1894	
12250	8.9119		9.9986		1.7607		1.0705		5.2521	
12500	9.3877		1.0446	4	1.8521		1.0764		5.3156	
12750	9.8792		1.0910		1.9525		1.0824		5.3800	
13000	1.0387	5	1.1390		2.0565		1.0885		5.4451	
13250	1.0910		1.1889		2.1583		1.0948		5.5110	
13500	1.1449		1.2407		2.2689		1.1012		5.5776	
13750	1.2006		1.2943		2.3771		1.1078		5.6449	
14000	1.2578		1.3501		2.4957		1.1146		5.7130	
14250	1.3167		1.4081		2.6189		1.1216		5.7819	
14500	1.3772		1.4682		2.7378		1.1288		5.8515	
14750	1.4395		1.5306		2.8685		1.1362		5.9218	
15000	1.5035		1.5958		3.0030		1.1439		5.9930	

Table 4. Total partition functions

T	CN		N_2		C_2		C		N	
	A	B	A	B	A	B	A	B	A	B
250	3.7336	32	9.9094	31	1.0373	32	4.8362	30	3.1967	30
500	4.2313	33	1.1209	33	2.1231	33	2.9694	31	1.8083	31
750	1.7797	34	4.6811		1.2952	34	8.4136		4.9832	
1000	5.0451		1.3131	34	4.6090		1.7515	32	1.0229	32
1250	1.1546	35	2.9725		1.2283	35	3.0856		1.7870	
1500	2.3055		5.8756		2.7368		4.8950		2.8189	
1750	4.1861		1.0566	35	5.3993		7.2263		4.1444	
2000	7.0834		1.7710		9.7559		1.0123	33	5.7864	
2250	1.1356	36	2.8108		1.6490	36	1.3628		7.7680	
2500	1.7442		4.2699		2.6451		1.7782		1.0109	33
2750	2.5876		6.2573		4.0674		2.2626		1.2830	
3000	3.7309		8.8976		6.0400		2.8202		1.5950	
3250	5.2519		1.2332	36	8.7097		3.4554		1.9488	
3500	7.2417		1.6720		1.2247	37	4.1724		2.3465	
3750	9.8088		2.2236		1.6853		4.9753		2.7901	
4000	1.3103	37	2.9078		2.2751		5.8687		3.2817	
4250	1.7193		3.7457		3.0206		6.8568		3.8236	
4500	2.2320		4.7613		3.9508		7.9439		4.4182	
4750	2.8645		5.9797		5.0989		9.1345		5.0684	
5000	3.6381		7.4291		6.5035		1.0433	34	5.7772	

Table 4. (Continued)

T	CN		N_2		C_2		C		N	
	A	B	A	B	A	B	A	B	A	B
5250	4.5756		9.1387		8.1950		1.1843		6.5467	
5500	5.7043		1.1142	37	1.0240	38	1.3369		7.3813	
5750	7.0528		1.3473		1.2672		1.5016		8.2840	
6000	8.6529		1.6168		1.5546		1.6789		9.2581	
6250	1.0541	38	1.9269		1.8929		1.8690		1.0308	34
6500	1.2752		2.2817		2.2885		2.0724		1.1437	
6750	1.5332		2.6857		2.7482		2.2896		1.2650	
7000	1.8325		3.1437		3.2800		2.5208		1.3952	
7250	2.1781		3.6609		3.8873		2.7667		1.5346	
7500	2.5750		4.2423		4.5926		3.0276		1.6837	
7750	3.0289		4.8944		5.3946		3.3038		1.8430	
8000	3.5463		5.6231		6.3037		3.5959		2.0131	
8250	4.1340		6.4345		7.3361		3.9042		2.1942	
8500	4.7980		7.3358		8.5018		4.2292		2.3872	
8750	5.5467		8.3343		9.8084		4.5712		2.5924	
9000	6.3876		9.4383		1.1279	39	4.9307		2.8103	
9250	7.3289		1.0655	38	1.2927		5.3082		3.0415	
9500	8.3811		1.1994		1.4761		5.7042		3.2865	
9750	9.5513		1.3464		1.6800		6.1188		3.5458	
10000	1.0851	39	1.5076		1.9070		6.5527		3.8202	

Table 4. (Continued)

T	CN A	CN B	N_2 A	N_2 B	C_2 A	C_2 B	C A	C B	N A	N B
10250	1.2290		1.6840		2.1572		7.0068		4.1099	
10500	1.3881		1.8769		2.4339		7.4811		4.4158	
10750	1.5634		2.0872		2.7443		7.9759		4.7383	
11000	1.7561		2.3165		3.0760		8.4916		5.0779	
11250	1.9678		2.5660		3.4508		9.0298		5.4353	
11500	2.1995		2.8373		3.8497		9.5908		5.8110	
11750	2.4528		3.1320		4.2991		1.0174	35	6.2059	
12000	2.7291		3.4518		4.7753		1.0783		6.6201	
12250	3.0301		3.7985		5.3104		1.1416		7.0546	
12500	3.3572		4.1740		5.8754		1.2073		7.5093	
12750	3.7123		4.5807		6.5083		1.2756		7.9861	
13000	4.0973		5.0201		7.1961		1.3466		8.4851	
13250	4.5135		5.4956		7.9205		1.4205		9.0066	
13500	4.9630		6.0095		8.7248		1.4972		9.5516	
13750	5.4488		6.5633		9.5700		1.5768		1.0120	35
14000	5.9714		7.1617		1.0510	40	1.6596		1.0715	
14250	6.5339		7.8072		1.1528		1.7455		1.1334	
14500	7.1378		8.5022		1.2587		1.8349		1.1980	
14750	7.7864		9.2506		1.3764		1.9276		1.2654	
15000	8.4815		1.0058	39	1.5028		2.0238		1.3355	

Table 5. Dissociation energies

N_2 (18)	9.759 eV
CN (18)	8.22 eV
C_2 (8,10,11,29)	6.13 eV

Table 6. Equilibrium constants (K_c)

	$N_2 \rightleftarrows 2N$		$C_2 \rightleftarrows 2C$		$CN \rightleftarrows C+N$	
T	A	B	A	B	A	B
250	1.4850	-193	4.6939	-120	6.6217	-163
500	4.9782	-95	2.6946	-58	7.2160	-80
750	3.8971	-62	9.3732	-38	3.7000	-52
1000	1.0467	-45	1.7048	-27	2.6926	-38
1250	7.7646	-36	2.4010	-21	5.5863	-30
1500	2.9460	-29	2.9768	-17	1.9473	-24
1750	1.4679	-24	2.4697	-14	1.7593	-20
2000	4.8717	-21	3.7795	-12	1.6191	-17
2250	2.6569	-18	1.8754	-10	3.2478	-15
2500	4.0920	-16	4.2309	-9	2.2417	-13
2750	2.5131	-14	5.3826	-8	7.1193	-12
3000	7.7471	-13	4.4573	-7	1.2626	-10
3250	1.4055	-11	2.6548	-6	1.4302	-9
3500	1.6820	-10	1.2209	-5	1.1395	-8
3750	1.4432	-9	4.5649		6.8497	
4000	9.4521		1.4437	-4	3.2696	-7
4250	4.9583	-8	3.9774		1.2983	-6
4500	2.1620	-7	9.7699		4.3994	
4750	8.0713		2.1791	-3	1.3073	-5
5000	2.6415	-6	4.4775		3.4743	
5250	7.7231		8.5861		8.3951	
5500	2.0492	-5	1.5475	-2	1.8684	-4
5750	4.9982		2.6483		3.8731	
6000	1.1327	-4	4.3304		7.5455	

Table 6. (Continued)

T	$N_2 \leftrightarrows 2N$		$C_2 \leftrightarrows 2C$		$CN \leftrightarrows C+N$	
	A	B	A	B	A	B
6250	2.4068		6.7987		1.3921	-3
6500	4.8303		1.0300	-1	2.4484	
6750	9.2173		1.5121		4.1263	
7000	1.6817	-3	2.1578		6.6964	
7250	2.9471		3.0064		1.0506	-2
7500	4.9814		4.0853		1.5990	
7750	8.1491		5.4429		2.3685	
8000	1.2943	-2	7.1215		3.4226	
8250	2.0013		9.1583		4.8358	
8500	3.0198		1.1599	0	6.6962	
8750	4.4558		1.4491		9.1010	
9000	6.4404		1.7868		1.2162	-1
9250	9.1352		2.1766		1.6001	
9500	1.2734	-1	2.6242		2.0752	
9750	1.7466		3.1322		2.6564	
10000	2.3603		3.7030		3.3592	
10250	3.1452		4.3437		4.2007	
10500	4.1370		5.0541		5.1983	
10750	5.3767		5.8258		6.3699	
11000	6.9083		6.6920		7.7366	
11250	8.7827		7.6149		9.3165	
11500	1.1055	0	8.6431		1.1133	0
11750	1.3785		9.7232		1.3206	
12000	1.7036		1.0923	1	1.5562	
12250	2.0878		1.2172		1.8218	
12500	2.5383		1.3543		2.1196	
12750	3.0635		1.4960		2.4524	
13000	3.6712		1.6464		2.8225	
13250	4.3698		1.8107		3.2328	
13500	5.1674		1.9797		3.6855	
13750	5.9355		2.1631		4.1817	
14000	7.1001		2.3503		4.7271	
14250	8.2509		2.5458		5.3213	
14500	9.5405		2.7599		5.9701	
14750	1.0979	1	2.9755		6.6738	
15000	1.2570		3.2013		7.4357	

Table 7. Comparison of the values of $-(F^\circ - E_o^\circ)/T$

	C_2		CN	
T(°K)	Altman (2)	Tveekrem	Johnston et al. (25)	Tveekrem
1000	49.796	49.8154	49.9789	49.9951
2500	57.837	57.8657	57.0219	57.0380
5000	64.175	64.2311	63.0738	63.0764

The results of these calculations were compared, when possible, with values available in the literature. Altman (2) and Johnston et al. (25) have calculated the thermodynamic functions for C_2 and CN respectively. They give values for the quantity $-(F^\circ - E_o^\circ)/T$ which is equal to R ln(Q/N). The partition functions obtained in this study for C_2 and CN were converted to values of $-(F^\circ - E_o^\circ)/T$ and a comparison of the results with those of Altman (2) and Johnston et al. (25) are shown in Table 7.

Pecker and Peuchot (46) have calculated the equilibrium constants for the dissociation of CN and N_2 assuming a harmonic oscillator and rigid rotator model for the molecules. A comparison of the log K_p (atmospheres) values of this study and those of Pecker and Peuchot is given in Table 8.

Table 8. Comparison of log K_p for CN and N_2

Pecker and Peuchot (46)			Tveekrem		
T(°K)	CN	N_2	T(°K)	CN	N_2
8400	1.404	1.208	8500	1.6695	1.3236
5040	-1.844	-2.862	5000	-1.8460	-2.9649
2520	-10.157	-12.898	2500	-10.3372	-13.0759
2016	-14.348	-17.883	2000	-14.5755	-18.0970

Fast (16) and Martinek (36) have made calculations for nitrogen in which the methods employed are quite comparable to the ones used in this study. A comparison of their values of K_p with the values obtained in this study is shown in Table 9.

Table 9. Comparison of K_p for dissociation of N_2

	Fast (16)		Martinek (36)		Tveekrem	
T(°K)	A	B	A	B	A	B
2000			7.51	-19	7.9975	-19
3000			1.75	-10	1.9077	-10
4000			2.62	-6	3.1034	-6
5000	1.07	-3	1.17	-3	1.0841	-3
6000	5.51	-2	5.42	-2	5.5787	-2
7000	9.56	-1	9.42	-1	9.6626	-1
8000	8.42		8.368		8.4994	
9000	4.72	1	4.6654	1	4.7578	1
10000	1.92	2	2.3007	2	1.9374	2

Concentrations of CN, N_2, C_2, C and N

The solution of the following set of simultaneous equations was required in order to obtain the relative concentrations of the atomic and molecular species as a function of temperature:

$$K_1 = [N]^2/[N_2] \quad (15)$$

$$K_2 = [C]^2/[C_2] \quad (16)$$

$$K_3 = [C][N]/[CN] \quad (17)$$

$$N_{total} = 2[N_2] + [N] + [CN] \quad (18)$$

$$C_{total} = 2[C_2] + [C] + [CN] \quad (19)$$

$$N_{total}/C_{total} = X \quad (20)$$

$$N_{total} = 2[N_2]_{original} \quad (21)$$

The brackets indicate the molar concentration of the various species. The $[N_2]_{original}$ is known and therefore N_{total} is known. Assuming X is known (as will be shown later), then C_{total} is also known from Equation 20. From Equations 15 and 16:

$$[N_2] = [N]^2/K_1 \quad (22)$$

$$[C_2] = [C]^2/K_2 \tag{23}$$

Substituting Equations 22 and 23 into Equations 18 and 19 yields:

$$N_{total} = (2[N]^2/K_1) + [N] + [CN] \tag{24}$$

$$C_{total} = (2[C]^2/K_2) + [C] + [CN] \tag{25}$$

Thus we now have three equations (17, 24 and 25) with three unknowns ([C], [N] and [CN]). Solution of Equation 17 for [CN] and substitution into Equations 24 and 25 yields two equations with two unknowns.

$$N_{total} = (2[N]^2/K_1) + [N] + ([C][N]/K_3). \tag{26}$$

$$C_{total} = (2[C]^2/K_2) + [C] + ([C][N]/K_3). \tag{27}$$

Solving Equation 27 for [N] gives:

$$[N] = (K_3/[C])\ (C_{total} - (2[C]^2/K_2) - [C]) \tag{28}$$

Substitution of Equation 28 into Equation 26 yields:

$$\begin{aligned} N_{total} = {} & (2K_3^2/K_1[C]^2)\ (C_{total} - (2[C]^2/K_2) - [C])^2 \\ & + (K_3/[C])\ (C_{total} - (2[C]^2/K_2) - [C]) \\ & + C_{total} - (2[C]^2/K_2) - [C] \end{aligned} \tag{29}$$

Multiplication of the factors in Equation 29 gives:

$$\begin{aligned} N_{total} = {} & (2K_3^2C_{total}^2/K_1[C]^2) - (8K_3^2C_{total}/K_1K_2) \\ & - (4K_3^2C_{total}/K_1[C]) + (8K_3^2[C]/K_1K_2) \\ & + (8K_3^2[C]^2/K_1K_2^2) + (2K_3^2/K_1) \\ & + (K_3C_{total}/[C]) - (2K_3[C]/K_2) \\ & - K_3 + C_{total} - (2[C]^2/K_2) - [C] \end{aligned} \tag{30}$$

Regrouping and factoring yields:

$$\begin{aligned} N_{total} = {} & (1/[C]^2)(2K_3^2C_{total}^2/K_1) \\ & + (1/[C])(C_{total})(K_3 - (4K_3^2/K_1)) \\ & + [C]\,((2K_3/K_2)\,((4K_3/K_1) - 1) - 1) \\ & + [C]^2(2/K_2)\,((4K_3^2/K_1K_2) - 1) \\ & + C_{total}(1 - (8K_3^2/K_1K_2)) + K_3((2K_3/K_1) - 1) \end{aligned} \tag{31}$$

The following simplifying substitutions are made:

$$W_1 = 2K_3^2C_{total}^2 / K_1 \tag{32}$$

$$W_2 = C_{total}(K_3 - (4K_3^2 / K_1)) \tag{33}$$

$$W_3 = (2K_3 / K_2)\,((4K_3 / K_1) - 1) - 1 \tag{34}$$

$$W_4 = (2 / K_2)\,((4K_3^2 / K_1K_2) - 1) \tag{35}$$

$$W_5 = C_{total}(1 - (8K_3^2 / K_1K_2)) + K_3((2K_3 / K_1) - 1) \tag{36}$$

These then yield:

$$(1/[C]^2)W_1 + (1/[C])W_2 + [C]W_3 + [C]^2W_4 + W_5 = 0 \qquad (37)$$

Multiplying by $[C]^2$ and dividing by W_4 yields:

$$[C]^4 + (W_3/W_4)[C]^3 + (W_5/W_4)[C]^2 + (W_2/W_4)[C] + (W_1/W_4) = 0 \qquad (38)$$

If we then let:

$$U_1 = W_3/W_4$$

$$U_2 = W_5/W_4$$

$$U_3 = W_2/W_4$$

$$U_4 = W_1/W_4$$

we arrive at:

$$[C]^4 + U_1[C]^3 + U_2[C]^2 + U_3[C] + U_4 = 0 \qquad (39)$$

An IBM 704 digital computer was employed to obtain the four roots of Equation 39 for each of the various temperature values. In every case three of the roots could be discarded because two were negative and one was greater than C_{total}. The remaining value of [C] for each value of T was then

substituted into Equation 28 to obtain a corresponding value of [N]. Knowing [C] and [N] as a function of temperature, the values of [CN], [C_2] and [N_2] were obtained by solution of Equations 15, 16 and 17.

The actual value of X was not known because the total amount of carbon in the discharge could not be accurately determined. Therefore, for each value of N_{total}, seven values of X (10^{-3}, 10^{-2}, 10^{-1}, 1, 10^{+1}, 10^{+2}, 10^{+3}) were used. Values of N_{total} corresponding to mixtures of 1.0 and 0.05% N_2 by volume in an inert gas at one atmosphere pressure were used in the calculations. The results indicated that for values of X greater than unity, the concentrations of the species varied directly with X (i.e., varying X by a factor of 10 changed the concentrations of the various species by a factor of 10 also). Thus if X was greater than unity, its absolute value would have no effect on the relative concentrations of the various species.

A crude measurement of X was made by introducing 1% by volume of nitrogen into one atmosphere of argon and arcing for measured time intervals between graphite electrodes. The weight loss of the electrodes was determined to be 0.001 gram per minute of arcing time. The dimensions of the discharge were approximately 6 mm in length by 3 mm in diameter. Assuming cylindrical symmetry this gave a discharge volume of approximately 0.043 cm^3. If an average temperature of

5000°K is assumed for the discharge, the molar volume of N_{total} will be 22420 x 5000/273 = 4.1 x 10^5 cm^3. N_{total} will then be equal to 0.01 x 4.3 x $10^{-2}/4.1 \times 10^5 = 1.05 \times 10^{-9}$ moles in the discharge volume.

In order to calculate the value of C_{total} in the discharge an assumption must be made about the length of time the carbon stays in the discharge. It will be assumed that all of the carbon vaporized from the electrodes passes through the discharge. Furthermore, after it leaves the discharge zone it will be assumed that it deposits as solid carbon on the chamber walls. The root-mean-square velocity, u, of carbon atoms can be calculated from the kinetic theory of gases by the following equation:

$$u = (3RT/M)^{1/2} = (3 \times 8.317 \times 10^7 \times 5 \times 10^3/12)^{1/2}$$

$$u = 3.2 \times 10^5 \text{ cm/sec}$$

Therefore a carbon atom could traverse the length of the arc in approximately 2 microseconds. Undoubtedly all of the carbon atoms do not travel the entire length of the arc; therefore, it will be assumed that the number of moles of carbon volatilized from the electrodes per microsecond is a conservative estimate of C_{total} in the discharge at any given instant. Therefore

$$C_{total} = 0.001/12 \times 60 \times 10^6 = 1.4 \times 10^{-12} \text{ moles}/\mu\text{sec}$$

Table 10. Concentration (moles/liter), 1% N_2 original

T	CN		N_2		C_2		C		N	
	A	B	A	B	A	B	A	B	A	B
1500	1.624	-7	8.114	-5	1.406	-12	6.470	-15	4.889	-17
1750	1.392		6.955		2.380		2.424	-13	1.010	-14
2000	1.218		6.085		3.472		3.622	-12	5.445	-13
2250	1.083		5.409		4.586		2.933	-11	1.199	-11
2500	9.730	-8	4.868		5.644		1.545	-10	1.411	-10
2750	8.800		4.426		6.556		5.940		1.055	-9
3000	7.942		4.057		7.177		1.789	-9	5.606	
3250	7.056		3.744		7.290		4.399		2.294	-8
3500	6.057		3.474		6.678		9.030		7.644	
3750	4.933		3.236		5.356		1.564	-8	2.161	-7
4000	3.778		3.017		3.706		2.313		5.340	
4250	2.729		2.806		2.268		3.004		1.180	-6
4500	1.893		2.588		1.269		3.521		2.365	
4750	1.281		2.347		6.797	-13	3.848		4.352	
5000	8.546	-9	2.067		3.607		4.019		7.389	
5250	5.632		1.741		1.937		4.078		1.159	-5
5500	3.653		1.375		1.068		4.065		1.679	
5750	2.313		1.001		6.060	-14	4.006		2.236	
6000	1.422		6.616	-6	3.546		3.919		2.738	

Table 10. (Continued)

T	CN		N_2		C_2		C		N	
	A	B	A	B	A	B	A	B	A	B
6250	8.492	-10	3.993		2.139		3.814		3.100	
6500	4.983		2.252		1.328		3.699		3.298	
6750	2.919		1.228		8.479	-15	3.581		3.364	
7000	1.731		6.664	-7	5.559		3.463		3.348	
7250	1.048		3.667		3.734		3.350		3.288	
7500	6.504	-11	2.065		2.573		3.242		3.208	
7750	4.136		1.194		1.811		3.140		3.120	
8000	2.695		7.101	-8	1.300		3.043		3.032	
8250	1.797		4.333		9.513	-16	2.952		2.945	
8500	1.224		2.711		7.079		2.865		2.861	
8750	8.509	-12	1.737		5.348		2.784		2.782	
9000	6.020		1.136		4.100		2.707		2.705	
9250	4.333		7.588	-9	3.187		2.634		2.633	
9500	3.169		5.162		2.506		2.564		2.564	
9750	2.351		3.578		1.994		2.499		2.499	
10000	1.767		2.514		1.603		2.436		2.436	
10250	1.345		1.797		1.301		2.377		2.377	
10500	1.036		1.302		1.065		2.321		2.321	
10750	8.064	-13	9.556	-10	8.818	-17	2.267		2.267	
11000	6.344		7.104		7.332		2.215		2.215	

Table 10. (Continued)

T	CN		N_2		C_2		C		N	
	A	B	A	B	A	B	A	B	A	B
11250	5.036		5.340		6.160		2.166		2.166	
11500	4.032		4.060		5.194		2.119		2.119	
11750	3.256		3.120		4.423		2.074		2.074	
12000	2.649		2.420		3.774		2.030		2.030	
12250	2.172		1.895		3.250		1.989		1.989	
12500	1.793		1.497		2.806		1.949		1.949	
12750	1.489		1.192		2.441		1.911		1.911	
13000	1.245		9.568	-11	2.134		1.874		1.874	
13250	1.046		7.740		1.868		1.839		1.839	
13500	8.840	-14	6.304		1.646		1.805		1.805	
13750	7.508		5.292		1.452		1.772		1.772	
14000	6.408		4.268		1.289		1.740		1.740	
14250	5.496		3.544		1.148		1.710		1.710	
14500	4.728		2.960		1.023		1.680		1.680	
14750	4.088		2.486		9.171	-18	1.652		1.652	
15000	3.549		2.099		8.242		1.624		1.624	

Table 11. Concentration (moles/liter), 0.05% N_2 original

T	CN		N_2		C_2		C		N	
	A	B	A	B	A	B	A	B	A	B
1500	8.122	-9	4.057	-6	7.031	-14	1.447	-15	1.093	-17
1750	6.961		3.477		1.190	-13	5.421	-14	2.259	-15
2000	6.090		3.043		1.736		8.099	-13	1.218	-13
2250	5.407		2.705		2.289		6.552	-12	2.681	-12
2500	4.838		2.434		2.791		3.437	-11	3.156	-11
2750	4.300		2.213		3.130		1.298	-10	2.358	-10
3000	3.689		2.028		3.098		3.716		1.253	-9
3250	2.931		1.870		2.517		8.175		5.127	
3500	2.087		1.731		1.591		1.394	-9	1.706	-8
3750	1.339		1.600		7.986	-14	1.909		4.805	
4000	8.058	-10	1.464		3.475		2.240		1.176	-7
4250	4.697		1.306		1.444		2.397		2.545	
4500	2.711		1.109		6.075	-15	2.436		4.896	
4750	1.541		8.647	-7	2.667		2.411		8.354	
5000	8.470	-11	5.927		1.235		2.352		1.251	-6
5250	4.423		3.446		6.035	-16	2.276		1.631	
5500	2.210		1.750		3.000		2.192		1.890	
5750	1.069		7.720	-8	1.678		2.108		1.964	
6000	5.267	-12	3.400		9.472	-17	2.025		1.962	

Table 11. (Continued)

T	CN		N_2		C_2		C		N	
	A	B	A	B	A	B	A	B	A	B
6250	2.683		1.529		5.573		1.947		1.918	
6500	1.423		7.164	-9	3.406		1.873		1.860	
6750	7.857	-13	3.504		2.153		1.804		1.797	
7000	4.511		1.792		1.403		1.740		1.736	
7250	2.685		9.563	-10	9.389	-18	1.680		1.679	
7500	1.649		5.293		6.458		1.624		1.624	
7750	1.043		3.032		4.540		1.572		1.572	
8000	6.776	-14	1.792		3.256		1.523		1.523	
8250	4.509		1.090		2.381		1.477		1.477	
8500	3.068		6.803	-11	1.771		1.433		1.433	
8750	2.130		4.351		1.338		1.392		1.392	
9000	1.507		2.845		1.025		1.354		1.354	
9250	1.084		1.899		7.969	-19	1.317		1.317	
9500	7.925	-15	1.291		6.267		1.282		1.282	
9750	5.878		8.940	-12	4.985		1.250		1.250	
10000	4.418		6.288		4.008		1.218		1.218	
10250	3.363		4.492		3.252		1.189		1.189	
10500	2.590		3.254		2.664		1.160		1.160	
10750	2.016		2.389		2.205		1.133		1.133	
11000	1.586		1.776		1.833		1.108		1.108	

Table 11. (Continued)

T	CN		N_2		C_2		C		N	
	A	B	A	B	A	B	A	B	A	B
11250	1.259		1.335		1.540		1.083		1.083	
11500	1.008		1.015		1.299		1.059		1.059	
11750	8.141	-16	7.7799	-13	1.106		1.037		1.037	
12000	6.623		6.050		9.436	-20	1.015		1.015	
12250	5.429		4.738		8.126		9.946	-10	9.946	-7
12500	4.482		3.742		7.014		9.747		9.747	
12750	3.723		2.980		6.103		9.555		9.555	
13000	3.112		2.392		5.334		9.372		9.372	
13250	2.615		1.935		4.669		9.195		9.195	
13500	2.210		1.576		4.114		9.025		9.025	
13750	1.877		1.323		3.629		8.861		8.861	
14000	1.602		1.067		3.281		8.702		8.702	
14250	1.374		8.859	-14	2.871		8.550		8.550	
14500	1.182		7.399		2.558		8.402		8.402	
14750	1.022		6.214		2.293		8.260		8.260	
15000	8.872	-17	5.248		2.061		8.122		8.122	

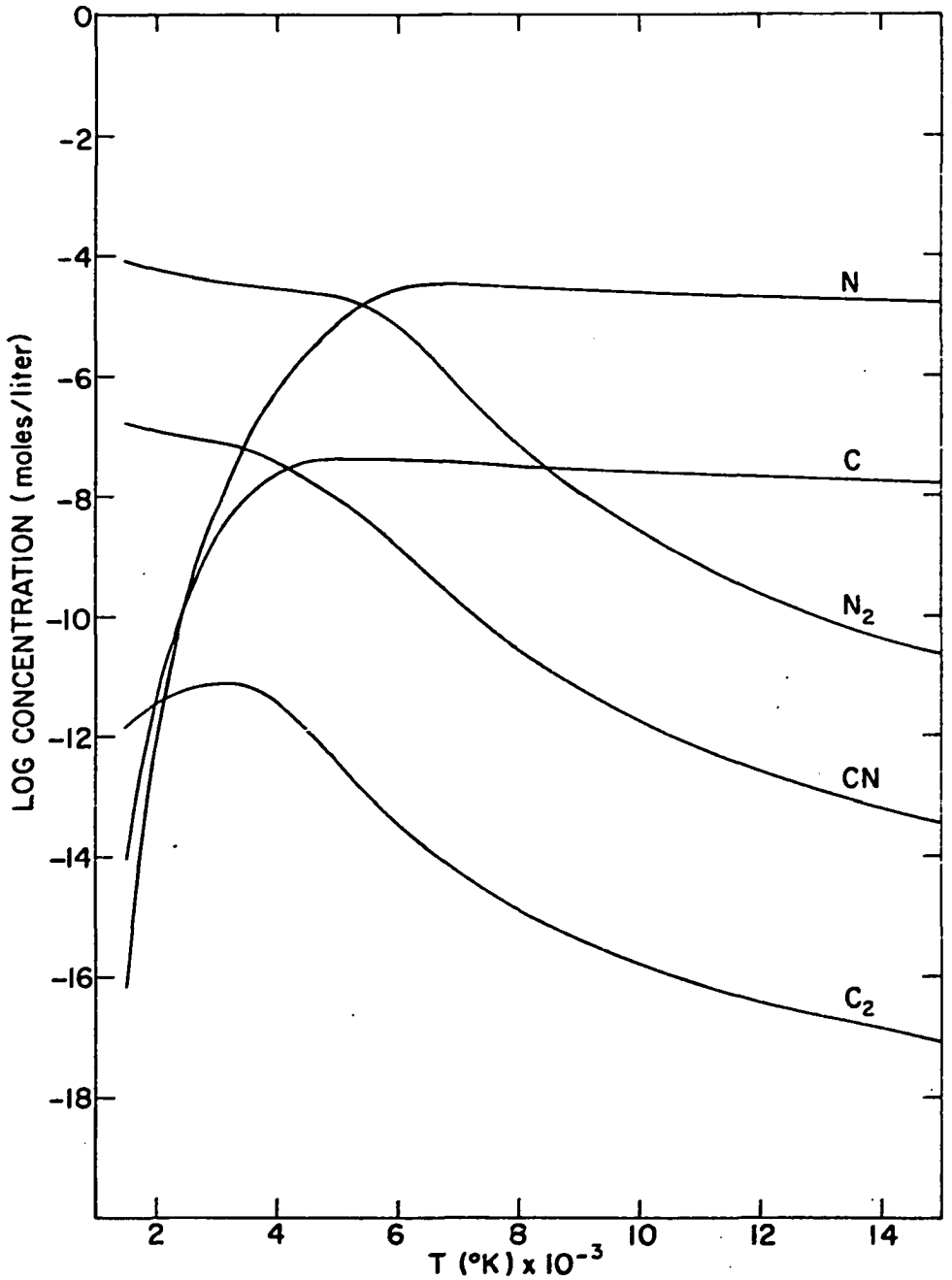

Figure 9. Concentrations of CN, N_2, C_2, C and N vs. temperature (1.0% N_2 original)

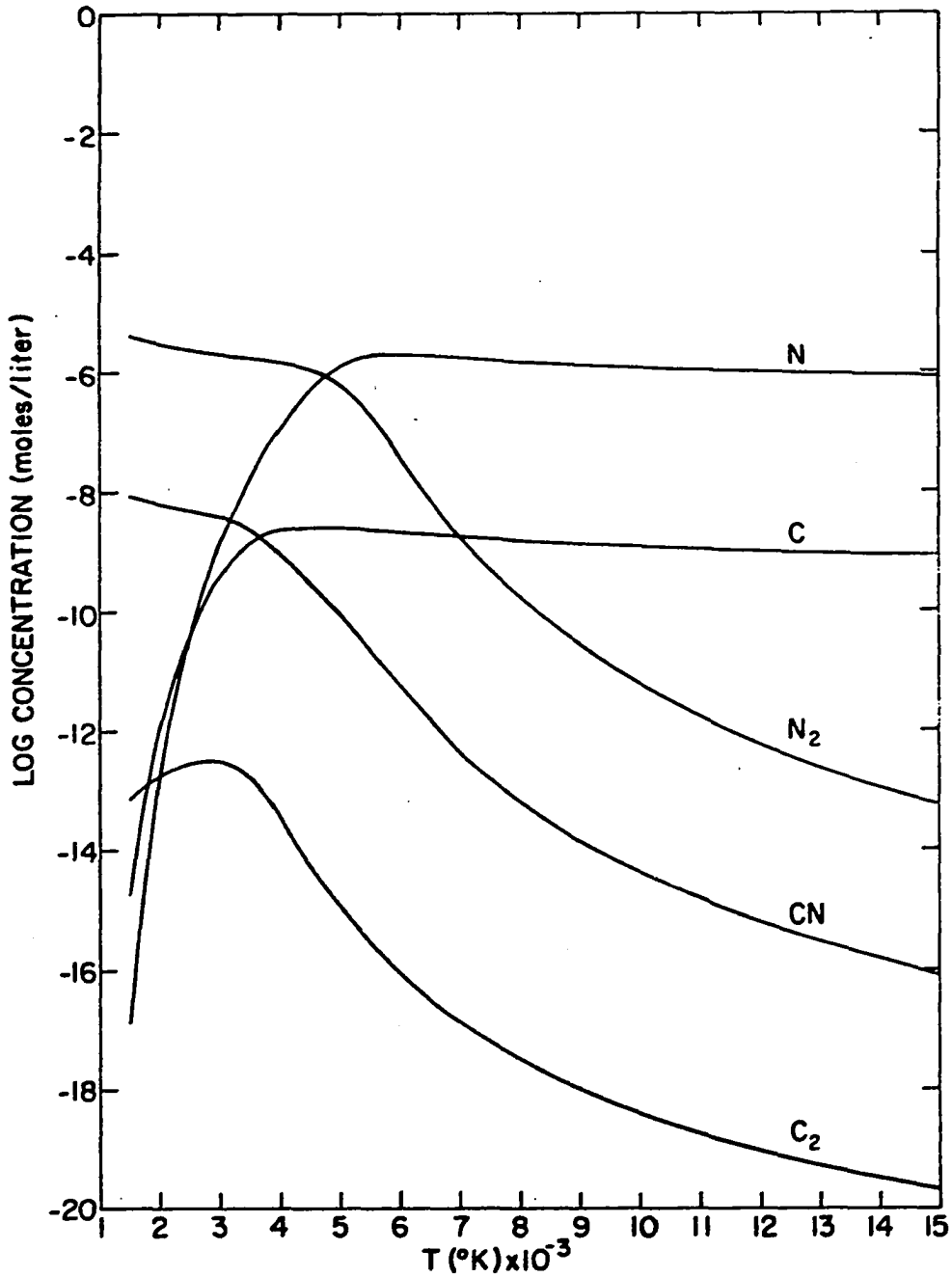

Figure 10. Concentrations of CN, N_2, C_2, C and N vs. temperature (0.05% N_2 original)

The value of X is then equal to

$$N_{total}/C_{total} = 1.05 \times 10^{-9}/1.4 \times 10^{-12} = 7.5 \times 10^{2}$$

Thus it was safe to assume that a large excess of nitrogen over carbon was present and the concentrations corresponding to the value of X equal to 10^3 were used. The concentrations of the five species as a function of temperature are listed in Table 10 for 1% $N_{2\ original}$ and in Table 11 for 0.05% $N_{2\ original}$. Curves representing these data are also shown in Figures 9 and 10.

Line Intensities

The intensity of a spectral line arising from a transition from upper energy state n to lower energy state m is given by the equation

$$I_{nm} = CN_n A_{nm} h\nu_{nm} c \qquad (40)$$

where

C = a constant depending on the units and geometry of the system

N_n = the number of emitting species with an electron in energy level n

A_{nm} = the Einstein transition probability for spontaneous emission (sec^{-1})

h = Planck's constant (erg sec)

ν = the energy difference between states n and m (cm^{-1})

c = the velocity of light ($cm\ sec^{-1}$)

If the generally accepted assumption is made that the energy levels of the emitter are populated according to the Boltzmann distribution, the following expression will be obtained for the number of emitters in the initial energy state of the transition:

$$N_{nm} = (g_n N_o / Q_{int.}) \exp(-E_n hc/kT) \quad (41)$$

In this equation

N_o = the total number of the emitting species

$Q_{int.}$ = the internal partition function

g_n = the degeneracy of the energy level n

E_n = the energy of the energy level n above the groundstate (cm^{-1})

T = the temperature of the system (°K)

The Einstein transition probability for spontaneous emission for the case of degenerate energy levels is defined as

$$A_{nm} = (64\pi^4 \nu_{nm}^3 / 3h)(\Sigma |R|^2 / g_n) \quad (42)$$

where $\Sigma |R|^2$ = the summation of the squares of the transition

matrix elements over all the possible combinations between the degenerate states n and m. For diatomic molecules this summation can be divided into its electronic, vibrational and rotational portions as follows:

$$\Sigma |R|^2 = \Sigma |R|_{el.}^2 \cdot \Sigma |R|_{vib.}^2 \cdot \Sigma |R|_{rot.}^2 \qquad (43)$$

The $\Sigma |R|_{rot.}^2$ is also known as the line strength, S_J, and is readily calculated from the total rotational angular momentum, J. The electronic and vibrational factors can only be obtained experimentally. For simplicity they will be designated $a_{el.}$ and $a_{vib.}$ hereafter.

The relative intensity of a spectral line for a diatomic molecule can then be given by the equation:

$$I_{nm} = (CN_o 64\pi^4 \nu_{nm}^4 a_{el.} a_{vib.} S_J / 3hQ_{int.}) \exp(-E_n hc/kT) \qquad (44)$$

The CN lines that are of interest in this thesis both involve the same electronic and vibrational transitions. The only difference is the rotational levels involved in the transitions. Therefore, since it is the intensity ratio that will be of interest, $a_{el.}$ and $a_{vib.}$ may be ignored because they will cancel when the intensity ratio is calculated.

The line strength formulae are given by Herzberg (20) and are listed below.

$$S_J \text{ (R branch)} = (J' + \Lambda')(J' - \Lambda')/J' \quad (45)$$

$$S_J \text{ (P branch)} = (J' + 1 + \Lambda')(J' + 1 - \Lambda')/J' + 1 \quad (46)$$

The CN lines arise from a $^2\Sigma - {}^2\Sigma$ electronic transition and therefore $\Lambda' = 0$. The equations then simplify to

$$S_J \text{ (R branch)} = J' \quad (47)$$

$$S_J \text{ (P branch)} = J' + 1 \quad (48)$$

The primes signify the upper or initial energy state of the transition and double primes will signify the lower or final energy state.

The energy E_n is given by $hcE(v';J')$, where $E(v';J')$ is the energy of level $(v';J')$ in units of cm^{-1}.

$$E(v';J') = E(v';0) + B_{v'}J'(J'+1) + D_{v'}J'^2(J'+1)^2 \quad (49)$$

The rotational analysis of the 0 - 0 band of the $^2\Sigma - {}^2\Sigma$ transition for CN has been done by Smit-Miessen and Spier (50). The following constants for determining the energies were obtained from their paper:

$$A = 25797.83 \pm 0.02 \text{ cm}^{-1}$$

$$B = 3.8501 \pm 0.0013 \text{ cm}^{-1}$$

$$C = 0.06774 \pm 0.00004 \text{ cm}^{-1}$$

$$D = (-12.96 \pm 0.185) \times 10^{-6} \text{ cm}^{-1}$$

$$F = (-23.8 \pm 0.7) \times 10^{-8} \text{ cm}^{-1}$$

$$E(v;0) = 0$$

where

$$A = E(v';0) - E(v;0) \tag{50}$$

$$B = B_{v'} + B_v \tag{51}$$

$$C = B_{v'} - B_v \tag{52}$$

$$D = D_{v'} + D_v \tag{53}$$

$$F = D_{v'} - D_v \tag{54}$$

Therefore:

$$B_{v'} = 1/2\ (B + C) \tag{55}$$

$$D_{v'} = 1/2\ (D + F) \tag{56}$$

$$E(v';0) = A \tag{57}$$

The energies for the P_{56} and R_{14} lines are thus given by:

$$E\ (P_{56}) = 25797.83 + (1.9589 \times 55 \times 56) - 6.60 \times 10^{-6}(55)^2(56)^2$$

$$= 31768.63 \text{ cm}^{-1}$$

$$E\ (R_{14}) = 25797.83 + (1.9589 \times 15 \times 16) - 6.60 \times 10^{-6}(15)^2(16)^2$$

$$= 26267.59 \text{ cm}^{-1}$$

A further consideration for calculating the intensities of these CN lines is the fact that they are all non- or partially resolved doublets. This arises because the electron orbital angular momentum is coupled with the internuclear axis whereas the electron spin angular momentum is not (Hund's case b). The nuclear rotation angular momentum couples with the electron orbital angular momentum to give a resultant angular momentum K. K is then coupled with the two possible values of the electron spin angular momentum to give two values ($K \pm 1/2$) for the total angular momentum J. The values of 14 and 56 given previously for J" are actually K" values and the J" values are 29/2, 27/2, 113/2 and 111/2. Thus the total line strength is 29/2 + 31/2 = 30 for the R_{14} lines and 113/2 + 111/2 = 112 for the P_{56} lines. This shows that S_J (R branch) = 2K' and S_J (P branch) = 2(K' + 1).

The final equations for calculating the relative intensities of the R_{14} and P_{56} lines for various temperatures are:

$$I(P_{56}) = (N_o/Q_{int.})\ 3.09012 \times 10^{33} \exp(-45708.77/T) \qquad (58)$$

$$I(R_{14}) = (N_o/Q_{int.})\ 8.37195 \times 10^{32} \exp(-37793.86/T) \qquad (59)$$

$$\log[I(P_{56})] = 33.48997 + \log(N_o) - \log(Q_{int.}) - 19851.07/T \qquad (60)$$

$$\log[I(R_{14})] = 32.92283 + \log(N_o) - \log(Q_{int.}) - 16413.67/T \qquad (61)$$

These relative intensities are listed in Tables 12 and 13.

The N_o in these equations corresponds to the concentration of CN as a function of T, which was calculated earlier, multiplied by the volume element of the discharge having a temperature of T $\pm$ 125°K. This volume element depends on the particular radial temperature distribution present in the discharge and is set equal to unity for all 250° temperature increments in the relative intensities listed in Tables 12 and 13.

The final column in these tables contains the intensity ratio P_{56}/R_{14} which would be obtained if the contributions from lower temperature regions are included in the total intensity of each line. These ratios were obtained by summing the intensities from each T = 250°K region (assuming equal volume elements for each region) up to temperature T, for each line and then taking the ratio of the two summations.

Comparison of the intensity ratios obtained in the two cases of 0.05% and 1.0% original N_2 revealed a surprising difference of values above 3000°K. It is apparent from the data in Tables 12 and 13 that the intensity ratio of the two CN lines increases as the initial nitrogen concentration is increased. Thus a variety of temperature values could be obtained by the simple expedient of varying the nitrogen concentration in the discharge.

Table 12. Relative intensities of CN lines, 1% N_2 original

T	P_{56} A	P_{56} B	R_{14} A	R_{14} B	$\frac{\Sigma I_{P_{56}}}{\Sigma I_{R_{14}}}$
1500	2.2652	10	1.2011	12	0.0189
1750	1.2221	12	3.0492	13	0.0393
2000	2.3097	13	3.2742	14	0.0678
2250	2.1791	14	1.9901	15	0.1031
2500	1.2649	15	8.1261		0.1439
2750	5.1578		2.4848	16	0.1887
3000	1.6032	16	6.0764		0.2362
3250	3.9906		1.2347	17	0.2851
3500	8.1654		2.1229		0.3340
3750	1.3934	17	3.1158		0.3815
4000	2.0110		3.9412		0.4261
4250	2.5229		4.4011		0.4671
4500	2.8264		4.4461		0.5042
4750	2.9120		4.1754		0.5373
5000	2.8133		3.7116		0.5664
5250	2.5737		3.1490		0.5917
5500	2.2344		2.5528		0.6131
5750	1.8354		1.9697		0.6306
6000	1.4247		1.4438		0.6445
6250	1.0490		1.0084		0.6549
6500	7.4351	16	6.8073	16	0.6625
6750	5.1655		4.5207		0.6681
7000	3.5747		3.0003		0.6720
7250	2.4898		2.0099		0.6749
7500	1.7554		1.3663		0.6770
7750	1:2538		9.4326	15	0.6785
8000	9.0830	15	6.6184		0.6796
8250	6.6719		4.7182		0.6805
8500	4.9656		3.4136		0.6812
8750	3.7434		2.5060		0.6817
9000	2.8531		1.8625		0.6821

Table 12. (Continued)

T	P_{56} A	P_{56} B	R_{14} A	R_{14} B	$\frac{\Sigma I_{P_{56}}}{\Sigma I_{R_{14}}}$
9250	2.1985		1.4015		0.6824
9500	1.7119		1.0670		0.6826
9750	1.3453		8.2080	14	0.6828
10000	1.0660		6.3732		0.6830
10250	8.5260	14	4.9959		0.6831
10500	6.8618		3.9507		0.6832
10750	5.5656		3.1487		0.6833
11000	4.5473		2.5299		0.6833
11250	3.7374		2.0463		0.6834
11500	3.0895		1.6659		0.6834
11750	2.5691		1.3652		0.6835
12000	2.1471		1.1251		0.6835
12250	1.8045		9.3287	13	0.6835
12500	1.5237		7.7761		0.6836
12750	1.2918		6.5111		0.6836
13000	1.1006		5.4817		0.6836
13250	9.4079	13	4.6320		0.6836
13500	8.0760		3.9327		0.6836
13750	6.9564		3.3515		0.6837
14000	6.0139		2.8677		0.6837
14250	5.2176		2.4635		0.6837
14500	4.5355		2.1210		0.6837
14750	3.9576		1.8338		0.6837
15000	3.4639		1.5907		0.6837

Table 13. Relative intensities of CN lines, 0.05% N_2 original

T	P_{56} A	P_{56} B	R_{14} A	R_{14} B	$\frac{\Sigma I_{P_{56}}}{\Sigma I_{R_{14}}}$
1500	1.1329	9	6.0068	10	0.0189
1750	6.1111	10	1.5248	12	0.0393
2000	1.1548	12	1.6371	13	0.0678
2250	1.0879	13	9.9359		0.1031
2500	6.2894		4.0405	14	0.1438
2750	2.5203	14	1.2141	15	0.1884
3000	7.4466		2.8225		0.2351
3250	1.6577	15	5.1290		0.2818
3500	2.8135		7.3147		0.3260
3750	3.7821		8.4575		0.3663
4000	4.2891		8.4061		0.4020
4250	4.3423		7.5749		0.4333
4500	4.0478		6.3673		0.4603
4750	3.5030		5.0229		0.4828
5000	2.7882		3.6786		0.5007
5250	2.0212		2.4730		0.5140
5500	1.3518		1.5444		0.5232
5750	8.4828	14	9.1034	14	0.5293
6000	5.2770		5.3476		0.5332
6250	3.3143		3.1861		0.5358
6500	2.1233		1.9440		0.5375
6750	1.3904		1.2168		0.5387
7000	9.3157	13	7.8189	13	0.5395
7250	6.3790		5.1493		0.5401
7500	4.4505		3.4641		0.5405
7750	3.1618		2.3787		0.5408
8000	2.2803		1.6616		0.5410
8250	1.6741		1.1839		0.5412
8500	1.2447		8.5563	12	0.5413
8750	9.3707	12	6.2731		0.5414
9000	7.1423		4.6625		0.5415

Table 13. (Continued)

T	P_{56} A	P_{56} B	R_{14} A	R_{14} B	$\frac{\Sigma I_{P_{56}}}{\Sigma I_{R_{14}}}$
9250	5.5000		3.5062		0.5416
9500	4.2810		2.6683		0.5416
9750	3.3635		2.0522		0.5416
10000	2.6654		1.5935		0.5417
10250	2.1301		1.2492		
10500	1.7155		9.8767	11	
10750	1.3914		7.8717		
11000	1.1368		6.3247		
11250	9.3434	11	5.1158		
11500	7.7238		4.1648		0.5418
11750	6.4236		3.4134		
12000	5.3683		2.8129		
12250	4.5103		2.3318		
12500	3.8088		1.9438		
12750	3.2299		1.6280		
13000	2.7511		1.3702		
13250	2.3520		1.1580		
13500	2.0190		9.8316	10	
13750	1.7391		8.3787		
14000	1.5035		7.1693		
14250	1.3044		6.1587		
14500	1.1339		5.3025		
14750	9.8940	10	4.5844		
15000	8.6593		3.9765		

Table 14. Spectral constants for the Ar and N lines

	A (sec^{-1})	g	E (cm^{-1})	ν (cm^{-1})
Ar 4259.36	2.46×10^6	1	118870.981	23471.099
Ar 4272.16	0.368×10^6	3	117151.387	23400.778
N 8629.24	28.1×10^6	4	97805.8	11585.324
N 8680.24	18.7×10^6	8	94883.1	11517.256

The calculation of the theoretical relative intensities of the argon and nitrogen lines necessitated the use of experimentally determined transition probabilities. The best values obtained thus far appear to be those of Olsen[1] for the argon lines and those of Richter (49) for the nitrogen lines. These values are listed in Table 14. Also included in this table are the values employed for the frequency, statistical weight of the initial energy level and energy of the initial level. The theoretical relative intensities of the nitrogen lines for various temperatures were then calculated from the following equations.

[1]Olsen, H. N., Speedway Laboratories, Linde Company, Division of Union Carbide Corp., Indianapolis, Indiana. Measurement of argon transition probabilities using the thermal arc plasma as a radiation source. Private communication. 1962.

$$I = ([N]gAv/Q_{int.}) \exp(-Ehc/kT) \quad (62)$$

$$\log(I_{N8629.24}) = 12.11468 + \log[N] - \log Q - 61115.312/T \quad (63)$$

$$\log(I_{N8680.24}) = 12.23629 + \log[N] - \log Q - 59289.016/T \quad (64)$$

The relative intensities of the nitrogen lines are listed in Tables 15 and 16 for the 1.0% and 0.05% original nitrogen cases respectively. The final column includes the theoretical summed intensity ratios assuming all volume elements are equal. These calculations were carried out only to 10000°K because, as will be shown in the following section, the maximum temperatures in the discharges appeared to be lower than this value. It will be noted that there is an insignificant concentration effect on the intensity ratios of these lines as contrasted to that obtained with the CN lines.

The relative intensities of the argon lines were calculated from the following equations.

$$\log(I_{Ar\ 4259.36}) = 10.76147 + \log[Ar] - 74278.174/T \quad (65)$$

$$\log(I_{Ar\ 4272.16}) = 10.41220 + \log[Ar] - 73203.660/T \quad (66)$$

In these cases the partition function was calculated using just the ground state term and therefore was equal to

unity at all temperatures. The argon concentration factor is simply the ideal gas law factor, P/RT, since there are no chemical equilibria involved. The concentration factors, relative intensities and intensity ratios are listed in Table 17. No effect due to the initial concentration of nitrogen on the intensity ratios would be expected. These values were also calculated only to 10000°K for the same reason as stated for the nitrogen lines.

Table 15. Relative intensities of nitrogen lines, 1.0% N_2 original

T	$I_{N8629.24}$ A	$I_{N8629.24}$ B	$I_{N8680.24}$ A	$I_{N8680.24}$ B	$\Sigma I_{N8629.24} / \Sigma I_{N8680.24}$
1500	2.8728	-46	6.2726	-45	0.046
1750	3.9256	-38	5.7427	-37	0.068
2000	4.9086	-32	5.3176	-31	0.092
2250	2.6859	-27	2.3034	-26	0.117
2500	1.6444	-23	1.1698	-22	0.141
2750	2.0516	-20	1.2526	-19	0.164
3000	7.7514	-18	4.1664	-17	0.186
3250	1.1703	-15	5.6471	-15	0.207
3500	8.5903	-14	3.7794	-13	0.227
3750	3.5412	-12	1.4381	-11	0.246
4000	9.1250	-11	3.4549	-10	0.263
4250	1.5951	-9	5.6767	-9	0.280
4500	2.0086	-8	6.7660	-8	0.296
4750	1.9126	-7	6.1337	-7	0.310
5000	1.4246	-6	4.3710	-6	0.324
5250	8.5096		2.5083	-5	0.337
5500	4.1535	-5	1.1805	-4	0.349
5750	1.6754	-4	4.6062		0.360
6000	5.6608		1.5096	-3	0.371
6250	1.6289	-3	4.2241		0.381
6500	4.0958		1.0349	-2	0.390
6750	9.2547		2.2831		0.399
7000	1.9258	-2	4.6464		0.407
7250	3.7546		8.8730		0.415
7500	6.9405		1.6088	-1	0.423
7750	1.2260	-1	2.7910		0.430
8000	2.0829		4.6617		0.438
8250	3.4156		7.5242		0.444
8500	5.4276		1.1778	0	0.451
8750	8.3858		1.7942		0.457
9000	1.2615	0	2.6633		0.463
9250	1.8541		3.8652		0.469
9500	2.6655		5.4908		0.474
9750	3.7580		7.6540		0.479
10000	5.1943		1.0466	1	0.484

Table 16. Relative intensities of nitrogen lines, 0.05% N_2 original

T	$I_{N8629.24}$ A	B	$I_{N8680.24}$ A	B	$\frac{\Sigma I_{N8629.24}}{\Sigma I_{N8680.24}}$
1500	6.4225	-47	1.4023	-45	0.046
1750	8.7801	-39	1.2844	-37	0.068
2000	1.0980	-32	1.1895	-31	0.092
2250	6.0057	-28	5.1505	-27	0.117
2500	3.6780	-24	2.6166	-23	0.141
2750	4.5854	-21	2.7997	-20	0.164
3000	1.7339	-18	9.3197	-18	0.186
3250	2.6160	-16	1.2624	-15	0.207
3500	1.9172	-14	8.4350	-14	0.227
3750	7.8740	-13	3.1977	-12	0.246
4000	2.0095	-11	7.6085	-11	0.263
4250	3.4403	-10	1.2243	-9	0.280
4500	4.1573	-9	1.4004	-8	0.295
4750	3.6714	-8	1.1774	-7	0.310
5000	2.4119	-7	7.4003		0.323
5250	1.1975	-6	3.5298	-6	0.336
5500	4.6755		1.3289	-5	0.348
5750	1.4716	-5	4.0458		0.359
6000	4.0564		1.0818	-4	0.369
6250	1.0084	-4	2.6148		0.379
6500	2.3099		5.8367		0.389
6750	4.9437		1.2196	-3	0.398
7000	9.9855		2.4092		0.406
7250	1.9173	-3	4.5309		0.415
7500	3.5135		8.1444		0.423
7750	6.1772		1.4062	-2	0.430
8000	1.0462	-2	2.3416		0.437
8250	1.7130		3.7736		0.444
8500	2.7185		5.8994		0.451
8750	4.1959		8.9774		0.457
9000	6.3146		1.3331	-1	0.463
9250	9.2738		1.9334		0.469
9500	1.3328	-1	2.7454		0.474
9750	1.8790		3.8270		0.479
10000	2.5971		5.2329		0.484

Table 17. Relative intensities of Ar lines

T	[Ar] A	[Ar] B	$I_{Ar\ 4259.36}$ A	$I_{Ar\ 4259.36}$ B	$I_{Ar\ 4272.16}$ A	$I_{Ar\ 4272.16}$ B	$\frac{\Sigma I_{Ar\ 4259.36}}{\Sigma I_{Ar\ 4272.16}}$
1500	8.1220	-3	1.4202	-41	3.3069	-41	0.429
1750	6.9615		1.4438	-34	2.6561	-34	0.544
2000	6.0915		2.5533	-29	3.9363	-29	0.649
2250	5.4145		3.0375	-25	4.0813	-25	0.744
2500	4.8732		5.4702	-22	6.5852	-22	0.831
2750	4.4302		2.4983	-19	2.7486	-19	0.909
3000	4.0610		4.0805	-17	4.1650	-17	0.979
3250	3.7486		3.0235	-15	2.8965	-15	1.043
3500	3.4809		1.2045	-13	1.0929	-13	1.101
3750	3.2488		2.9220	-12	2.5290	-12	1.153
4000	3.0458		4.7384	-11	3.9355	-11	1.201
4250	2.8666		5.5159	-10	4.4174	-10	1.245
4500	2.7073		4.8726	-9	3.7780	-9	1.285
4750	2.5649		3.4121	-8	2.5703	-8	1.321
5000	2.4366		1.9617	-7	1.4396	-7	1.356
5250	2.3206		9.5247		6.8274		1.387
5500	2.2151		3.9971	-6	2.8043	-6	1.416
5750	2.1188		1.4778	-5	1.0168	-5	1.444
6000	2.0305		4.8907		3.3052		1.469

Table 17. (Continued)

T	[Ar] A	[Ar] B	$I_{Ar\ 4259.36}$ A	$I_{Ar\ 4259.36}$ B	$I_{Ar\ 4272.16}$ A	$I_{Ar\ 4272.16}$ B	$\frac{\Sigma I_{Ar\ 4259.36}}{\Sigma I_{Ar\ 4272.16}}$
6250	1.9493		1.4684	-4	9.7609		1.493
6500	1.8743		4.0449		2.6482	-4	1.515
6750	1.8049		1.0322	-3	6.6630		1.536
7000	1.7404		2.4601		1.5674	-3	1.556
7250	1.6804		5.5159		3.4717		1.575
7500	1.6244		1.1706	-2	7.2845		1.592
7750	1.5720		2.3640		1.4555	-2	1.609
8000	1.5229		4.5643		2.7823		1.625
8250	1.4767		8.4594		5.1088		1.640
8500	1.4333		1.5107	-1	9.0435		1.654
8750	1.3924		2.6080		1.5482	-1	1.667
9000	1.3537		4.3638		2.5703		1.680
9250	1.3171		7.0960		4.1487		1.692
9500	1.2824		1.1239	0	6.5249		1.704
9750	1.2496		1.7377		1.0021	0	1.715
10000	1.2183		2.6267		1.5052		1.726

RESULTS AND DISCUSSION

The mean values of the experimentally determined P_{56}/R_{14} intensity ratios are listed in Table 18. Both the peak and area intensity ratios are included along with their standard deviations. The mean value of fifteen determinations of the factor for converting the peak intensity ratios to area intensity ratios was 1.689 ± 0.0061.

The standard deviations of these mean values were calculated according to the formula (7):

$$\sigma_{\bar{x}} = \left[\left(\sum_{i=1}^{N} (x_i - \bar{x})^2\right) / N(N-1)\right]^{1/2} \qquad (67)$$

The standard deviation of the product (1.689 ± 0.0061) x (peak intensity ratio) was obtained from the formula:

$$\sigma_{\bar{x}\bar{y}} = \bar{x}\bar{y}\left[(\sigma_{\bar{x}}/\bar{x})^2 + (\sigma_{\bar{y}}/\bar{y})^2\right]^{1/2} \qquad (68)$$

It will be noted that there is a considerable variation in the P_{56}/R_{14} intensity ratio when the initial nitrogen concentration is varied from 0.05% to 1.0%, as was predicted in the theoretical intensity calculations. If no radial concentration distribution or radial temperature distribution were considered for the discharges it would then appear that they possessed quite different temperatures. However, it is

Table 18. Experimental intensity ratios of the CN lines

Atmosphere	Number of determinations	P_{56}/R_{14} (peak)	P_{56}/R_{14} (area)
0.05% N_2 in Ar	9	0.452 ± 0.0095	0.763 ± 0.0183
1.0 % N_2 in Ar	11	0.647 ± 0.0080	1.093 ± 0.0184
0.05% N_2 in He	11	0.492 ± 0.0061	0.831 ± 0.0140
1.0 % N_2 in He	10	0.666 ± 0.0092	1.125 ± 0.0202

a more plausible assumption that the small amounts of nitrogen present in the discharges in either of the two initial concentrations will have no significant effect on the temperature. The temperature of the discharge will be largely controlled by the characteristics of the rare gas atmosphere. Therefore, the radial concentration and temperature distributions must be the source of the variable intensity ratios.

The final column in Tables 12 and 13 listed the theoretical intensity ratios as a function of the maximum temperatures of the discharge if the radial temperature distribution was such that all $\Delta T = 250°$ zones had equal volumes. In this case the intensity ratio leveled off at approximately 0.54 for the 0.05% N_2 and 0.68 for the 1.0% N_2 initial concentrations. These values are considerably lower than those obtained experimentally. It would thus appear that some

other radial temperature distribution must exist in the discharges being studied.

Huldt (24) employed a radial temperature distribution of the form $T = T_o / (1 + r^4)$ where T_o is the maximum temperature and r is proportional to the radius. The form of this distribution is shown in Figure 11. In applying this or any other radial temperature distribution, it must be realized that the experimental optical system is such that the entire diameter of the discharge is focussed on the spectrograph collimator. Therefore, an end-on view of the discharge may be visualized as a series of concentric zones corresponding to different temperatures. If we wish to calculate the relative volumes at 500° temperature increments, it is only necessary to obtain the values of the difference of the squares of the radii at T ± 250°K. The intensity at temperature T is then multiplied by its corresponding volume element and all of these corrected intensities summed up to the maximum temperature to obtain the total relative intensity of the particular spectral line.

Using the radial distribution from Huldt's paper, the relative radii were calculated for the respective cases of T_o equal to 6000, 7000, 8000, 9000 and 10000°K. The relative volumes were then calculated at intervals of 500° from 1500° to T_o. The corrected intensities were summed over this temperature range to obtain the P_{56}/R_{14} intensity ratios for

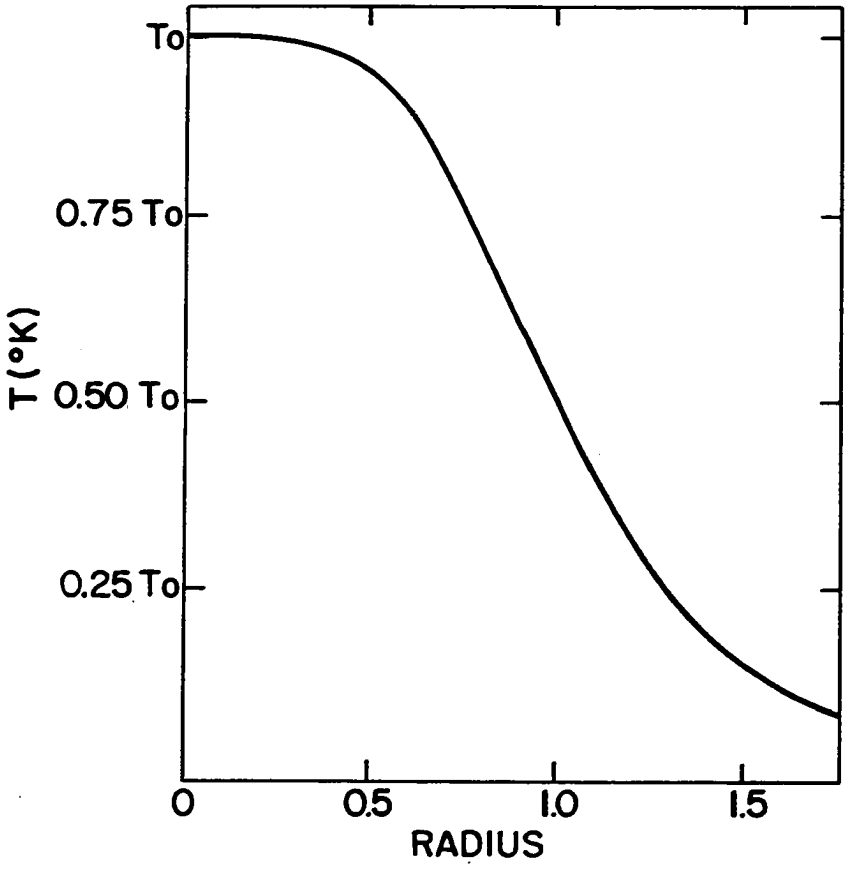

Figure 11. Radial temperature profile described by the equation $T = T_o / (1 + r^4)$

Table 19. Theoretical CN intensity ratios for various values of T_o using radial temperature distribution of Huldt (24)

T_o	P_{56}/R_{14} (0.05% N_2)	P_{56}/R_{14} (1.0% N_2)
10000	0.503	0.638
9000	0.506	0.644
8000	0.511	0.653
7000	0.518	0.663
6000	0.531	0.665

these distributions. The values obtained are listed in Table 19 for both cases of 0.05% and 1.0% initial nitrogen concentration.

Obviously this radial temperature distribution is far from that required to accurately portray the situation present in these discharges. The intensity ratios are hardly affected by large changes in the maximum temperature and never approach the values obtained experimentally.

A study of the non-volume-corrected intensities in Tables 12 and 13 in conjunction with the relative volume elements for this distribution listed in Table 20 immediately shows the reason for this behavior. The relative volume elements change very little, within one order of magnitude, with respect to temperature for this distribution. However, the

Table 20. Relative volume elements calculated for different values of T_o from the radial temperature distribution given by Huldt (24)

T	T_o=6000°	T_o=7000°	T_o=8000°	T_o=9000°	T_o=10000°
1500	.3910	.4127	.4340	.4546	.4745
2000	.2674	.2791	.2912	.3034	.3153
2500	.2039	.2098	.2169	.2245	.2322
3000	.1673	.1690	.1728	.1774	.1825
3500	.1453	.1432	.1444	.1469	.1502
4000	.1329	.1366	.1253	.1260	.1278
4500	.1287	.1161	.1122	.1113	.1119
5000	.1350	.1109	.1034	.1008	.1001
5500	.1695	.1111	.0982	.0933	.0915
6000	.2085	.1199	.0964	.0885	.0851
6500		.1540	.0988	.0860	.0807
7000		.1924	.1087	.0861	.0780
7500			.1420	.0897	.0771
8000			.1796	.1001	.0783
8500				.1325	.0826
9000				.1690	.0932
9500					.1246
10000					.1601

intensities of the lines vary by several orders of magnitude, with the maximum intensities prevailing in the temperature range of approximately 4000 - 6000°K. Therefore it can be expected that the total intensity of the spectral lines will be dominantly controlled by the emission from these relatively cool zones of the discharges. In order to obtain the relatively high intensity ratios observed experimentally, a distribution must be present so that the volume elements from the higher temperature central portions of the discharge are several orders of magnitude higher than those from the temperature regions of less than 6000 - 7000°K. This type of distribution would feasibly be similar to that of Figure 12 where line B indicates a large temperature gradient near the perimeter of the discharge and line A signifies a small temperature gradient throughout the main column of the discharge. The slopes of the two lines, A and B, can be varied and the effect on the theoretical intensity ratios noted. The slopes of the lines are defined in units of 1000°/0.1 of the distance from the axis to the intersection of lines A and B.

The relative volume elements from the distribution in Figure 12 were calculated by employing a stepwise approximation of the distribution at 1000° intervals with T_o set equal to 10000°K. The slope of line A was set arbitrarily at 0.2 and the intensity ratios, P_{56}/R_{14}, calculated for slopes of line B equal to 10, 25 and 50. The intensity ratios

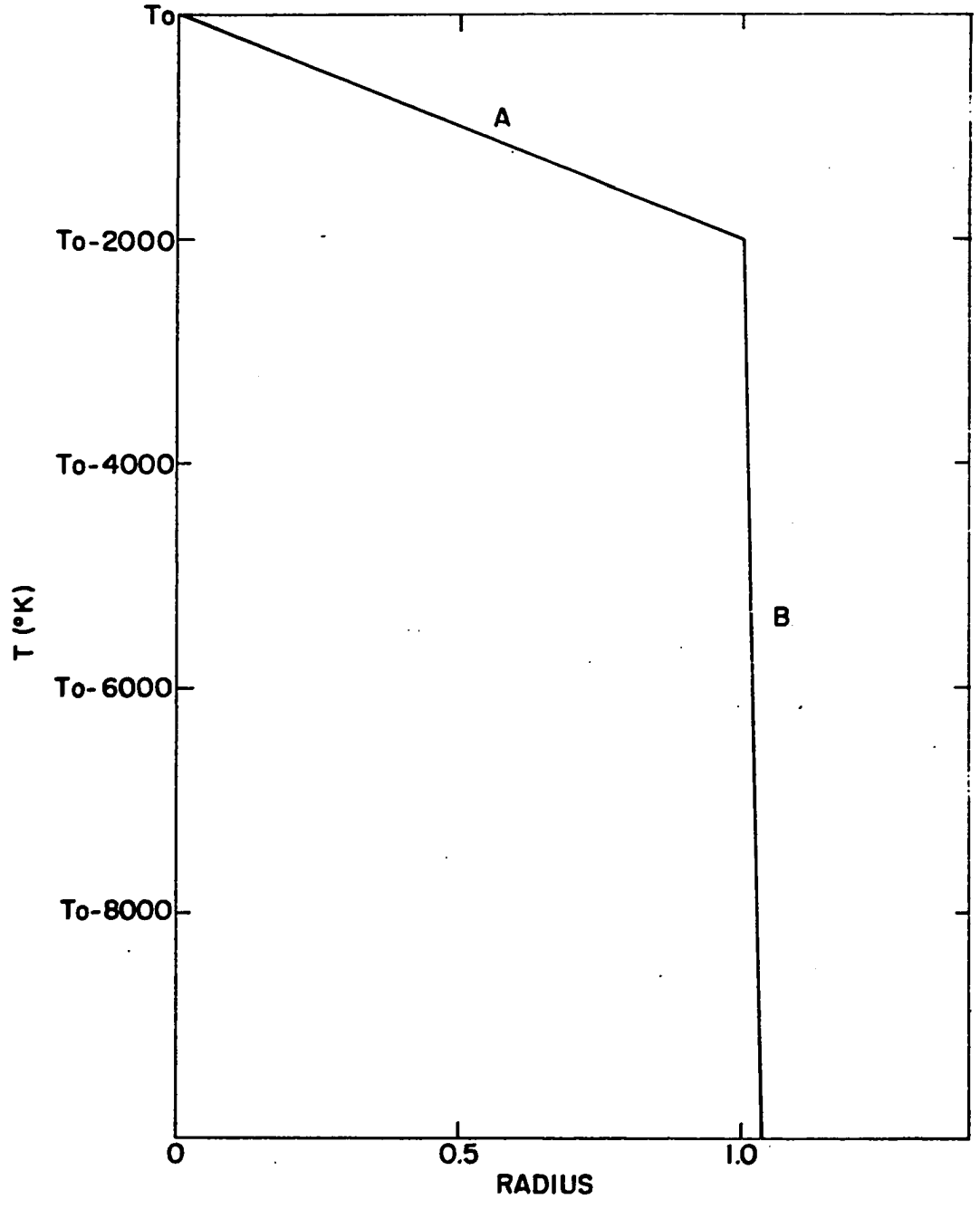

Figure 12. Basic radial temperature profile where the slopes of lines A and B may be varied

calculated in this manner for 0.05% N_2 and 1.0% N_2 originally present are tabulated in Table 21. It can be seen that the intensity ratios are approaching the experimental values as the slope of line B is increased.

The slope of line B was then set at 50 and the intensity ratios calculated for slope of line A equal to 0, 0.1, 0.2, 0.3, 0.4 and 0.5. These results are listed in Table 22. This shows a considerable range of values for the intensity ratios with a peak in the vicinity of slope A = 0.3. In fact, the values obtained for slope A = 0.3 and slope B = 50 correspond very nearly to the experimental ones for the argon discharges.

This distribution was then refined further by varying the slope at 500° intervals of line A as shown in Figure 13. The slopes of the segments are 1/8, 1/6, 1/4 and 1/2. The slope of line B was maintained at 50 and a series of intensity ratios calculated using 500° intervals for the volume elements and varying the maximum temperature. These results are listed in Table 23.

Recalling from Table 18 that the experimental intensity ratios in argon discharges were 0.76 ± 0.02 and 1.09 ± 0.02 for the 0.05% and 1.0% $N_{2\ original}$ respectively, it can be seen from perusal of Table 23 that a maximum temperature of 9000°K will correspond very closely to these data. In the case of helium discharges the experimental intensity ratios

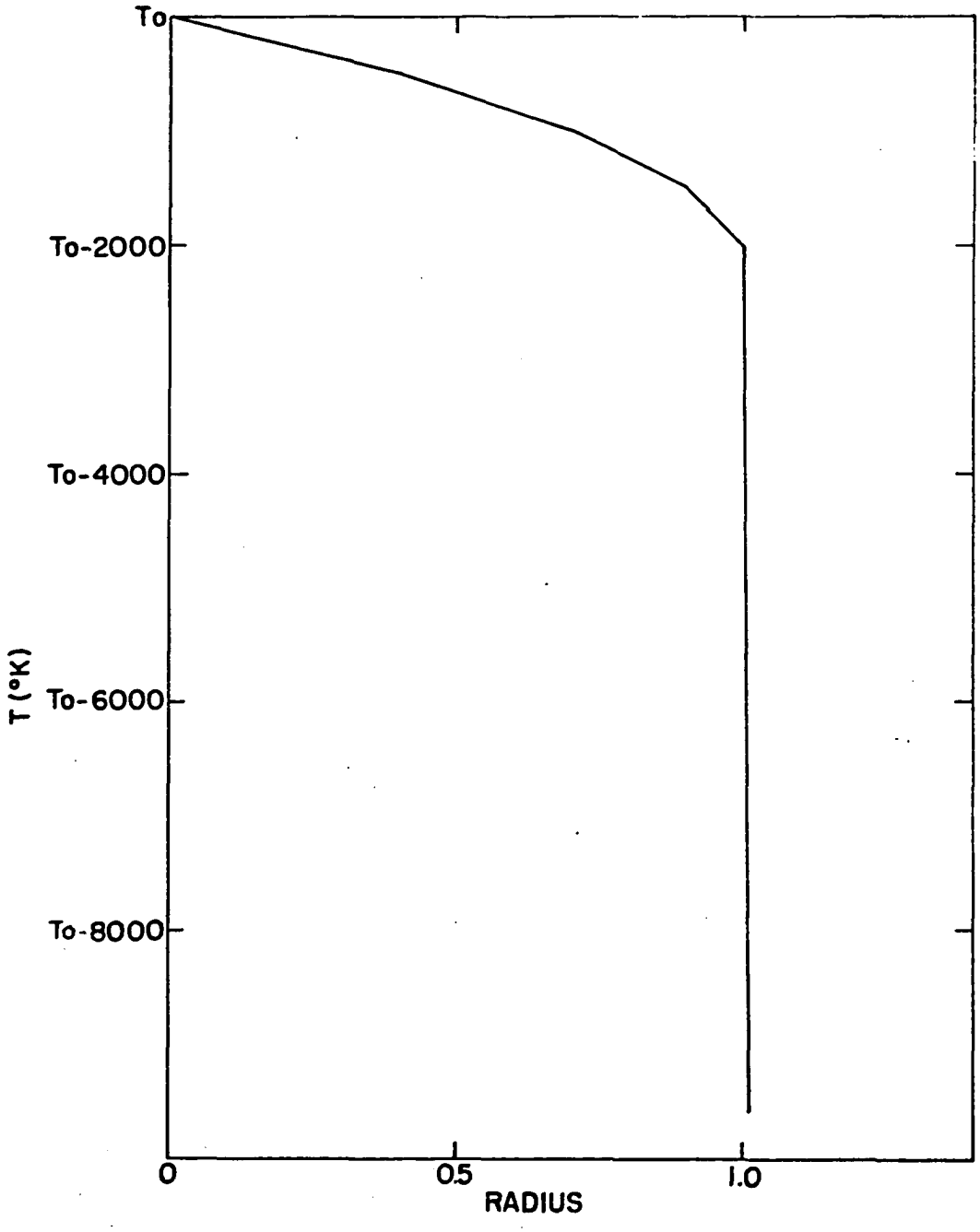

Figure 13. Final radial temperature profile employed in the calculations

Table 21. Theoretical CN intensity ratios obtained from the application of the radial temperature distribution in Figure 12 (slope of line A = 0.2 and slope of line B varied)

Slope of line B	$I_{P_{56}}/I_{R_{14}}$ (0.05% N_2)	$I_{P_{56}}/I_{R_{14}}$ (1.0% N_2)
10	0.568	0.792
25	0.606	0.915
50	0.660	1.038

Table 22. Theoretical CN intensity ratios obtained from the application of the radial temperature distribution in Figure 12 (slope of line B = 50 and slope of line A varied)

Slope of line A	$I_{P_{56}}/I_{R_{14}}$ (0.05% N_2)	$I_{P_{56}}/I_{R_{14}}$ (1.0% N_2)
0	0.573	0.816
0.1	0.603	0.921
0.2	0.660	1.038
0.3	0.782	1.107
0.4	0.897	1.022
0.5	0.795	0.867

Table 23. Theoretical CN intensity ratios as a function of T_o obtained from application of the radial temperature distribution shown in Figure 13

T_o	$I_{P_{56}}/I_{R_{14}}$ (0.05% N_2)	$I_{P_{56}}/I_{R_{14}}$ (1.0% N_2)
10000	0.624	0.980
9500	0.675	1.061
9000	0.752	1.113
8500	0.846	1.113
8000	0.915	1.064
7500	0.932	0.989

were 0.83 ± 0.014 and 1.125 ± 0.02 respectively and Table 23 indicates that these data closely correspond to a maximum temperature of 8500°K.

It was also noted from Table 22 that the argon discharges could have a maximum temperature of 10000°K if the radial distribution of Figure 12, with line A having a slope of 0.3 and line B a slope of 50, was employed for the calculation of the theoretical intensity ratios. Furthermore, there are undoubtedly other possibilities of attaining agreement with the experimental data by applying slight modifications to this basic radial temperature distribution. Therefore, without a precise knowledge of the radial temperature distribution present in the discharge, the maximum temperature cannot be precisely determined.

Unfortunately, there is no good method of measuring the radial temperature distribution in these discharges because of their poor spatial stability. The generally recognized method of obtaining the temperature distribution has been that of Larenz (31). This method has been employed by numerous investigators as noted in the Introduction. However, in all cases it has been applied to high current arcs or plasma jets possessing good spatial stability. Also, emission from high energy lines has generally been utilized in these studies and it appears to be highly doubtful that the method could be employed using a low energy species such as CN.

Although it cannot be proved experimentally, the basic radial temperature distribution employed for the arc discharges studied in this work does fit the data reasonably well. It is not unreasonable to expect a precipitous decline in temperature at the edge of the discharge, and the relatively flat temperature profile in the center of the discharge is in harmony with distributions reported for higher current discharges in rare gases.

The intensity ratios of N8629.24Å/N8680.24Å and Ar 4259.36Å/Ar 4272.16Å were also calculated and measured in order to check the validity of the results obtained with CN. The radial temperature distribution shown in Figure 13 was employed for the calculations. The calculated intensity ratios are shown as a function of the maximum temperature in Table 24.

The experimentally determined values of the N8629.24Å/N8680.24Å intensity ratios were 0.359 ± 0.0065 for helium and 0.385 ± 0.0056 for argon discharges. This resulted in maximum temperatures of approximately 6000°K for the helium and 6500°K for the argon discharges.

The experimental value of the Ar 4259.36Å/Ar 4272.16Å intensity ratio was determined in the same manner as the CN intensity ratios because the argon lines were quite diffuse and also asymmetric. The mean value of 25 determinations of the peak intensity ratio was 1.131 ± 0.0040 and the mean

Table 24. Calculated intensity ratios of nitrogen and argon lines using the radial temperature distribution shown in Figure 13

T_o	$I_{N8629.24}/I_{N8680.24}$	$I_{Ar\ 4259.36}/I_{Ar\ 4272.16}$
10000	0.480	1.708
9500	0.469	1.689
9000	0.457	1.667
8500	0.444	1.641
8000	0.430	1.612
7500	0.415	1.579
7000	0.399	1.541
6500	0.381	1.498
6000	0.363	1.452
5500	0.343	1.403
5000	0.323	1.352

value of 10 determinations of the area/peak ratio was 1.185 ± 0.0165. The resultant area intensity ratio was 1.340 ± 0.0209. Table 24 indicates that this value corresponds to a maximum temperature of approximately 5000°K.

The values of T_o obtained with the different thermometric species through the utilization of the radial temperature distribution shown in Figure 13 are compared in Table 25. There is no semblance of agreement among the values and at first glance it would appear that the assumption of the existence of thermodynamic equilibrium was grossly in error. However,

Table 25. Comparison of T_o values obtained with different thermometric species

Thermometric species	Helium	Argon
CN	8500°K	9000°K
N	6000°K	6500°K
Ar		5000°K

it is instructive at this point to compare the values of the average temperatures that would be obtained from the data if no radial concentration or temperature distributions had been considered. These are listed in Table 26.

In this situation the temperature values are in much better agreement with one another when different species are employed as "thermometers" but it is impossible to reconcile the large difference in temperatures obtained when the same species (CN) is used at two different concentrations in the discharges. Furthermore, when the radial concentration distributions of CN in conjunction with a very plausible radial temperature distribution (Figure 13) are utilized, unique maximum temperatures of the discharges are obtained from the CN data, independent of the CN concentration. It should be recalled that the transition probabilities of the nitrogen and argon lines were experimentally determined values and thus susceptible to experimental errors. The error in each

Table 26. Comparison of average temperatures obtained from various thermometric species if no radial concentration or temperature distributions are considered

Thermometric species	Helium	Argon
CN (0.05% N_2)	5310°K	5020°K
CN (1.0% N_2)	6660°K	6500°K
N	5650 °K	6160°K
Ar		4840°K

of the nitrogen line transition probabilities was estimated by Richter (49) to be ±15%. If each of these errors were utilized in opposing directions the theoretical intensity ratios of the nitrogen lines could be decreased as much as 26%. Referring to Table 24 it will be noted that a decrease of the theoretical intensity ratios by only 16-19% would give values of T_o of 8500° and 9000°K for the helium and argon discharges, in consort with those obtained from CN.

For the argon transition probabilities, Olsen (see footnote on page 75) estimated the error to be ± 9% for the Ar 4259.36 line and ±5% for the Ar 4274.16 line. Utilizing these error estimates to their maximum would decrease the calculated argon intensity by 13.5%. This correction would not attain the T_o of 9000°K which is sought for the argon discharge but it would bring T_o up to nearly 7500°K. An

additional error of 6% would bring the results into agreement with those of CN and N. Although it is not a good practice to assume maximum errors in reported measurements in order to bring about agreement in experimental results, it is well recognized that rather large errors are oftentimes associated with the values of transition probabilities available in the literature. Thus it is entirely possible that the discharges studied in this work had a radial temperature distribution similar to that shown in Figure 13, with maximum temperatures of approximately 8500°K for helium and 9000°K for argon atmospheres.

It should be emphasized that the results of this thesis all indicate that an accurate temperature determination of these arc discharges presupposes a precise knowledge of the radial temperature distribution. Even if the discharge were very stable, the precipitous decline in temperature at the edge of the discharge could not be accurately measured. This region would be relatively unimportant if high energy species were being used as the "thermometers" but the lines of these species have the disadvantage that knowledge of their transition probabilities is rather inaccurate. The rotational lines of molecular spectra can be used to advantage here because their transition probabilities can be accurately calculated. However, the energies of the molecular species tend to restrict them mainly to the peripheral region of the discharge,

thus necessitating an accurate knowledge of the temperature distribution in this region.

It is thus quite apparent that any method of temperature measurements on electrical discharges must take into consideration both the concentration distribution of the thermometric species and the temperature distribution of the discharge.

Another uncertainty in temperature measurement of electrical discharges is whether there actually is local thermodynamic equilibrium present in the discharge. The numerous studies made on arc discharges in air have established with certainty that local thermodynamic equilibrium does exist in these arcs at atmospheric pressure. As indicated in the Introduction of this thesis, some investigators have questioned whether thermal equilibrium is attained in rare gas arc discharges at atmospheric pressure.

The calculations and measurements in this thesis were based on the assumption that local thermodynamic equilibrium was present in these rare gas discharges. Although the results obtained do not definitely prove this assumption, the fact that the various intensity measurements with different species can be made to give a reasonably unique maximum temperature by proper application of radial temperature distribution goes far toward indicating that no severe departure from equilibrium is likely.

SUGGESTIONS FOR FUTURE WORK

There are numerous possibilities for further work on temperature measurements in rare gas arc discharges.

The most important aspect of these studies should be the accurate determination of the radial temperature distribution prevalent in these discharges. If the discharges can be stabilized, either by special electrode geometries or by constricting the plasma in some manner, measurements could be made in a manner similar to that described in the Introduction, as applied to high current arcs and plasma jets.

If an accurate radial temperature distribution can be determined, then the methods employed in this thesis can be applied to the calculation of the radial concentration profiles of some other system containing diatomic molecules. The molecule, CO, would be of special interest because it is the most stable common diatomic molecule.

A further refinement of the calculations employed in this thesis could be made by considering the ionization equilibria. This would necessitate a knowledge of the electron concentration in the arc plasma. Methods employing the measurement of the broadening of spectral lines (particularly those of hydrogen) have recently been utilized for this purpose (57). The ionization equilibria would have a small effect, on the order of 1%, on the concentrations (36) of

most species below temperatures of 9000-10000°K.

If the temperatures and radial temperature distributions of rare gas arc discharges were accurately known, these discharges could be employed for the measurement of the transition probabilities of spectral lines for numerous species. A small amount of a metal could be volatilized into the discharge and, assuming the presence of the metal atoms did not perturb the temperature distribution, the line intensities from the metal atoms could be measured and their transition probabilities determined.

In most of the suggestions listed here, the utilization of a "direct-reader" spectrograph would have distinct advantages. These are a decrease in the time required to make intensity measurements and an increase in the precision of the experimental data. To obtain accurate integrated line intensities it would be necessary to provide the instrument with a wavelength scanning device.

SUMMARY

A study of conditions necessary for accurate temperature measurements of low current (25-30 ampere) atmospheric pressure d.c. arc discharges in argon and helium atmospheres has been made. Small amounts of carbon and nitrogen introduced into the discharges supplied the species required for thermometric measurements. It was recognized that both the radial concentration distributions of the thermometric species and the radial temperature distributions of the discharges were necessary parameters for accurate temperature determinations.

It was assumed that local thermodynamic equilibrium existed in the arc column and three chemical equilibria were treated.

$$N_2 \leftrightarrows 2N$$

$$C_2 \leftrightarrows 2C$$

$$CN \leftrightarrows C+N$$

The partition functions of the above five species and, subsequently, the equilibrium constants for the three dissociation reactions were calculated at 250° intervals to 15000°K. The concentrations of the five species were then obtained as a function of temperature through the solution of a system of simultaneous equations.

The radial temperature distribution of the discharges could not be measured because of the spatial instability of

the arc column. However, several plausible types of temperature distributions were assumed and the results obtained when they were utilized were discussed.

The intensity ratios of CN rotational lines, nitrogen atomic lines and argon atomic lines were measured from observations on the entire discharge diameter. These were then compared with the theoretically calculated integrated intensity ratios, which included contributions from all the temperature zones in the discharge.

It was discovered that an accurate knowledge of the radial temperature distribution of the arc column was necessary to obtain definitive temperature measurements. A temperature distribution was found which gave reasonable agreement among the data obtained with several thermometric species. A maximum temperature of 9000°K for the argon discharges and 8500°K for the helium discharges was found to fit the data. However, the possibility of other radial temperature distributions and, correspondingly, other maximum temperatures could not be eliminated.

A definitive answer to the question of the existence of local thermodynamic equilibrium in rare gas arc discharges could not be made from the results obtained in this work.

BIBLIOGRAPHY

1. Adelstein, S. J. and Vallee, B. L., Spectrochim. Acta 6, 134 (1954).

2. Altman, R. L., J. Chem. Phys. 32, 615 (1960).

3. Andermann, G. and Kemp, J. W., Am. Soc. Testing Mater., Spec. Tech. Publ. 259, 23 (1960).

4. Aston, J. G. and Fritz, J. J. Thermodynamics and statistical thermodynamics. New York, N. Y., John Wiley and Sons, Inc. 1959.

5. Baker, M. R., Adelstein, S. J. and Vallee, B. L., J. Opt. Soc. Am. 46, 138 (1956).

6. Ballik, E. A. and Ramsay, D. A., J. Chem. Phys. 31, 1128 (1959).

7. Beers, Y. Introduction to the theory of error. 2nd ed. Reading, Mass., Addison-Wesley Publishing Co., Inc. 1957.

8. Brewer, L., Hicks, W. J. and Krikorian, O. H., J. Chem. Phys. 36, 182 (1962).

9. Burhorn, F., Maecker, H. and Peters, T., Z. Phys. 131, 28 (1951).

10. Drowart, J., Burns, R. P., DeMaria, G. and Inghram, M. G., J. Chem. Phys. 31, 1131 (1959).

11. _____ and Honig, R. E., J. Phys. Chem. 61, 980 (1957).

12. Druyvesteyn, M. J. and de Groot, W., Physica 12, 153 (1932).

13. Dumond, J. W. M. and Cohen, E. R. Fundamental constants of atomic physics. In Condon, E. U. and Oldishaw, H., eds. Handbook of physics. pp. 7-143 - 7-173. New York, N. Y., McGraw-Hill Book Co., Inc. 1958.

14. Egorov, V. N., Kolesnikov, V. N. and Sobolev, N. N., Soviet Phys. - Dokl. 3, 775 (1958).

15. Fassel, V. A., Iron and Steel Inst. (London), Spec. Rept. 68, 103 (1960).

16. Fast, J. D., Philips Res. Rept. 2, 382 (1947).

17. Finkelnburg, W. and Maecker, H. Elektrische Bögen und thermisches Plasma. In Flügge, S., ed. Handbuch der Physik. Vol. 22, Gasentladungen 2. pp. 254-444. Berlin, Springer-Verlag. 1956.

18. Gaydon, A. G. Dissociation energies. 2nd ed. rev. London, Chapman and Hall, Ltd. 1953.

19. Hammaker, E. M., Pope, G. W., Ishida, Y. G. and Wagner, W. F., Appl. Spectr. 12, 161 (1958).

20. Herzberg, G. Spectra of diatomic molecules. 2nd ed. New York, N. Y., D. Van Nostrand Co., Inc. 1950.

21. Herzfeld, C. M., J. Wash. Acad. Sci. 46, 269 (1956).

22. Hörmann, H., Z. Phys. 97, 539 (1935).

23. Hottel, H. C., Williams, G. C. and Jensen, W. P. Optical methods of measuring plasma jet temperatures. U. S. Atomic Energy Commission Report WADD TR 60-676. [Aeronautical Systems Division, Air Force Systems Command, United States Air Force, Wright-Patterson Air Force Base, Ohio], 1961.

24. Huldt, L., Spectrochim. Acta 7, 264 (1955).

25. Johnston, H. L., Belzer, J. and Savedoff, L. Thermodynamic properties of CN between 1° and 6000° computed from spectroscopic data. U. S. Atomic Energy Commission Report AD 13734. [Cryogenic Laboratory, Department of Chemistry, The Ohio State University, Columbus, Ohio], 1953.

26. Jurgens, G., Z. Phys. 134, 21 (1952).

27. _____, Z. Phys. 138, 613 (1954).

28. Knopp, C. F., Gottschlich, C. F. and Cambel, A. B. A spectroscopic technique for the measurement of temperature in transparent plasmas. U. S. Atomic Energy Commission Report AF OSR-1100. [Gas Dynamics Laboratory, Northwestern University, Evanston, Illinois], 1961.

29. Knox, B. E. and Palmer, H. B., Chem. Rev. 61, 247 (1961).

30. Kostkowski, H. J., Intern. Symposium High Temp. Technol., Asilomar Conf. Grounds, Calif. Proc. 1959, 33 (1960).

31. Larenz, R. W., Z. Phys. 129, 327 (1951).

32. _____, Z. Phys. 129, 343 (1951).

33. Lochte-Holtgreven, W., Rept. Progr. Phys. 21, 312 (1958).

34. Maecker, H., Z. Phys. 129, 108 (1951).

35. _____, Z. Phys. 135, 13 (1953).

36. Martinek, F. Nitrogen at high temperatures. U. S. Atomic Energy Commission Report AF OSR TN-59-264. [Flight Propulsion Laboratory Department, General Electric Company, Cincinnati, Ohio], 1959.

37. Marzuvanov, V. L., Bull. Acad. Sci. USSR, Phys. Ser. 23, 1051 (1959).

38. _____, Vestn. Akad. Nauk Kaz. SSR 16, 85 (1960).

39. Mastrup, F. and Wiese, W., Z. Astrophys. 44, 259 (1958).

40. Mochalov, K. N. and Raff, E. L., Soviet Phys.-Tech. Phys. 1, 487 (1957).

41. Moore, C. E., Nat. Bur. Std. (U. S.), Circ. 467, 21 (1949).

42. Mulliken, R. S. The energy levels of the nitrogen molecule. In Zelikoff, M., ed. The threshold of space. pp. 169-179. New York, N. Y., Pergamon Press. 1957.

43. Olson, H. N., Bull. Am. Phys. Soc., Ser. 2, 6, 390 (1961).

44. Ornstein, L. S. and Brinkman, H., Physica 1, 797 (1934).

45. Pearce, W. J. Plasma jet temperature study. U. S. Atomic Energy Commission Report WADC TR 59-346. [Wright Air Development Division, Air Research and Development Command, United States Air Force, Wright-Patterson Air Force Base, Ohio], 1960.

46. Pecker, J. C. and Peuchot, M., Mem. Soc. Roy. Sci. Liege, Ser. 4, 18, 352 (1957).

47. Pitzer, K. S. Quantum chemistry. New York, N. Y., Prentice-Hall, Inc. 1953.

48. Preining, O. The attainment of high temperatures (up to 55,000°) under laboratory conditions. U. S. Atomic Energy Commission Report AEC-tr-2369. [Associated Technical Services, East Orange, New Jersey], 1956.

49. Richter, J., Z. Astrophys. 51, 177 (1961).

50. Smit-Miessen, M. M. and Spier, J. L., Physica 9, 193 (1942).

51. Sobolev, N. N., Kolesnikov, V. N. and Kitaeva, V. F., Intern. Conf. Ionization Phenomena Gases, Uppsala. Proc. 4, 370 (1959).

52. Stone, H., J. Opt. Soc. Am. 44, 411 (1954).

53. Thiers, R. E., Appl. Spectr. 7, 157 (1953).

54. Vallee, B. L. and Baker, M. R., J. Opt. Soc. Am. 46, 77 (1956).

55. _____ and _____, J. Opt. Soc. Am. 46, 83 (1956).

56. Wall, F. T. Chemical thermodynamics. San Francisco, California., W. H. Freeman and Co. 1958.

57. Wiese, W. L., and Shumaker, J. B., Jr., J. Opt. Soc. Am. 51, 937 (1961).

ACKNOWLEDGMENTS

The author wishes to express his gratitude to Dr. V. A. Fassel for his patience and encouragement throughout this investigation and especially for his invaluable suggestions during the writing of this manuscript.

A great indebtedness to Mr. Richard N. Kniseley is acknowledged both for suggesting this problem and for the many helpful discussions in which he participated.

Thanks are also extended to Mr. Aaron Booker and Mrs. Harriet Spanel for their efforts in providing the digital computer solutions required in this investigation.

Finally, the author wishes to extend a special thanks to his wife, Carol, without whose patience and understanding this investigation could not have been completed.